

Topology in Chemistry: Designing Möbius Molecules†

Rainer Herges*

Otto-Diels-Institut für Organische Chemie, Universität Kiel, D-24118 Kiel, Germany

Received August 1, 2006

Contents

1. Introduction	4820
2. Non-conjugated Molecular Möbius Strips	4822
3. Möbius π Systems	4824
3.1. Theoretical Calculations	4824
3.1.1. Annulenes	4824
3.1.2. Cyclacenes	4829
3.1.3. Kekulene and Other Coronoid Structures	4830
3.1.4. Other Möbius Systems	4831
3.1.5. Möbius Transition States	4831
3.2. Design and Synthesis of the First Möbius Annulene	4832
4. Double Twisted π Systems	4839
5. References	4841

1. Introduction

In 1747, Johann Sebastian Bach wrote a series of canons and fugues on the occasion of his visit to King Frederick the Great of Prussia in Potsdam. His music of homage, the “Musikalisches Opfer” (Musical Offering, BWV1079), includes a canon that is probably one of the oldest man-made examples of an object with Möbius topology.¹ The canon canonicans (crab canon) is written for two violins playing the same score in two different directions. If you cut the score, paste it in such way that it forms a band with the notes of the first violin on top and those of the second violin below, fold it lengthwise between the two notes, give one end a half twist, and join both ends, you end up with an endless Möbius-shaped score (Figure 1). After every turn the two violins change their parts. Karl Amadeus Hartmann, Nicolas Slonimsky,² and others several centuries later wrote further examples of Möbius music.

Note that there are two different ways to form the Möbius score, by twisting the strip either clockwise or anticlockwise. The two Möbius strips are enantiomers (the music, unfortunately, is not) and exhibit the highest symmetry a Möbius object can attain: C_2 .

More than 100 years later, August Ferdinand Möbius and Johann Benedict Listing (Figure 2), both students of Carl Friedrich Gauss in Göttingen, published their seminal work on projective planes and one-sided surfaces. Nowadays, the credit goes almost exclusively to Möbius³ after whom the famous band is named, even though Listing published 4 years earlier.⁴ Both mathematicians mentioned the “Möbius” band in unpublished papers for the first time in 1858; however,



Rainer Herges was born in St. Ingbert, Saarland (now Germany), in 1955. He studied Chemistry at the University of the Saarland, Saarbrücken, and moved to the Technical University of Munich, where he obtained his Ph.D. degree in 1984 under Prof. Ivar Ugi. After 1 year as a postdoc at the University of Southern California with Professor George Olah, he joined the group of Prof. P. v. R. Schleyer at the University of Erlangen for habilitation. He received a C3 position as Professor at the Institute for Organic Chemistry at the Technical University Braunschweig in 1996, and in 2001 he was appointed a Full Professorship of Organic Chemistry at the University of Kiel. His research interests range from Theoretical Chemistry to the synthesis of “non-natural” compounds. Most projects are a combination of theoretical methods and preparative chemistry, such as the synthesis of tubelike aromatics, Möbius annulenes, photoswitchable systems, and anion selective sensors. The theoretical work includes investigations of magnetic properties, developments for the elucidation of structure and reactivity of biologically active systems, and the theory of coarctate transition states.

again Listing’s unpublished note (July) predates the one of Möbius (September) by 2 months.

It would probably be fair to name the one-sided band a “Listing band”. There are good reasons to assume that Listing was not adequately credited because of social rather than scientific reasons.⁵

Most of the objects we are dealing with in our everyday lives are two-sided. They have an inside and an outside surface like a sphere, a cube, or a torus. This is also true for most two-dimensional mathematical objects. According to the mathematical definition, a normal vector on the surface of a two-sided object cannot be shifted to any other point on the surface without crossing a border or interpreted in anthropomorphic terms: walking upright on the outside surface you cannot enter the inside and vice versa. The Möbius band is probably the simplest and best-known exception (Figure 3). Any closed band with an odd number of 180° twists is one-sided, and those with an even number of 180° twists are two-sided.

Unfortunately, the sidedness is not an intrinsic property, because it requires that the surface is embedded in a

† In memory of Professor Edgar Heilbronner.

* To whom correspondence should be addressed. Telephone: ++49 431 880 2440. Fax: ++49 431 880 1558. E-mail: rherges@oc.uni-kiel.de.



Johann Sebastian Bach



Figure 1. Johann Sebastian Bach and the score of the “canon cancrizans” for two violins. The left portion is reprinted with permission from Baerenreiter-Verlag/Gustav Bosse Verlag.



August Ferdinand Möbius
1790-1866



Johann Benedict Listing
1808-1882

Figure 2. August Ferdinand Möbius and Johann Benedict Listing.

surrounding space. Thus, a closed curve that has an inside and outside in two dimensions is no-sided in three-dimensional space. Orientability is an intrinsic and more generally applicable property. A surface is called orientable if it is not possible to move a shape on the surface in such a way that it is transformed into its mirror image, which is true for two-sided objects. However, consider the Fischer formula of D-lactic acid drawn on a (transparent) Möbius band. If you move the structure around the band, the stereochemistry is reversed and it returns as its mirror image L-lactic acid and upside-down. This means that the Möbius band is non-orientable (Figure 4).

The notion of orientability is also applicable to higher-dimensional spaces. For example, in a non-orientable three-

dimensional universe there would be a path along which a bottle of D-lactic acid could be carried so that it would return as L-lactic acid. (Because this has not been observed, there is empirical evidence that we live in an orientable universe.)

Imagine a Möbius band made from rubber and try to move all points on the edge toward each other, you would end up with the so-called “projective plane”, which has no edge. In three dimensions a geometrical realization is difficult. It took till 1903 when Werner Boy found a geometric realization of the projective plane.⁷ Another non-orientable surface that is easier to construct (albeit with self-intersection in the 3D-projection) is the Klein bottle (Figure 5).⁸ If you cut the Klein bottle along the mirror plane, you obtain two Möbius bands, which are enantiomers.

§ 11. Von der verschiedenartigen Form der zweierlei Zonenflächen kann man sich eine sehr anschauliche Vorstellung mittelst eines Papierstreifens verschaffen, welcher die Form eines Rechtecks hat. Sind A, B, B', A' die vier Ecken desselben in ihrer Aufeinanderfolge, und wird er hierauf gebogen, so dass die Kante $A'B'$ sich stets parallel bleibt, bis sie zuletzt mit AB zusammenfällt, so erhält der Streifen die Form einer Cylinderfläche, also einer zweiseitigen Zone, welche die zwei nunmehr kreisförmigen Kanten AA' und BB' des anfänglichen Rechtecks, zu ihren zwei Grenzlinien hat. — Man kann aber auch, dafern das eine Paar paralleler Kanten AA' und BB' gegen das andere AB und $A'B'$ hinreichend gross ist, A' mit B , und B' mit A zur Coincidenz bringen, indem man zuvor, das eine Ende AB des Streifens festhaltend, das andere Ende $A'B'$ um die Längsaxe des Streifens halb herumdreht, als wodurch $A'B'$ mit BA einerlei Richtung erhält. Die nach der letztgedachten Coincidenz entstandene Fläche hat nur Eine Grenzlinie, nämlich die aus den jetzt gebogenen und in A und B' , sowie in B und A' an einander grenzenden Linien AA' und BB' zusammengesetzte. Auch hat diese Fläche nur Eine Seite; denn wenn man sie — um dieses noch auf andere Weise vorstellig zu machen — von einer beliebigen Stelle aus mit einer Farbe zu überstreichen anfängt und damit fortfährt, ohne mit dem Pinsel über die Grenzlinie hinaus auf die andere Seite überzugehen, so werden nichtsdestoweniger zuletzt an jeder Stelle die zwei daselbst einander gegenüberliegenden Seiten der Fläche gefärbt seyn.

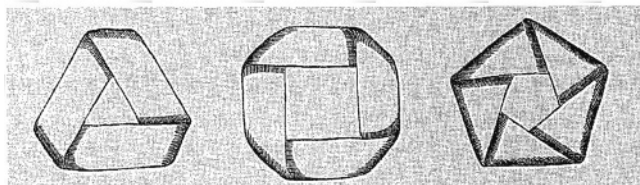


Figure 3. (Top) Möbius' original recipe to construct a Möbius band.³ “One can, however, ...superpose A' with B , and B' with A , by holding the side AB fixed, give the other end $A'B'$ a half-twist... The surface created by this superposition has only one edge ... and one side.” (Bottom) More twisted bands from Möbius' unpublished writings.⁶

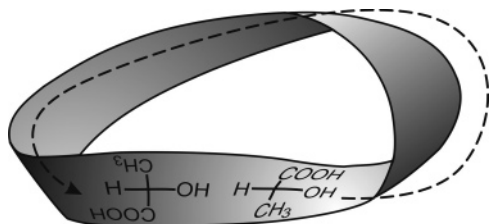


Figure 4. A Möbius band is non-orientable. The Fischer formula of D-lactic acid drawn on the (transparent) surface is transformed into the mirror image (L-lactic acid) by moving it around the Möbius band.

Examples of molecules with orientable and non-orientable surfaces and diagrams in the usual vector notation are given in Figure 6.

Möbius, Listing, and Klein inspired a number of artists to create sculptures and drawings of non-orientable surfaces.⁹ Among the most famous Möbius artworks probably are the Möbius sculptures of the Swiss architect and sculptor Max Bill and the Dutch graphic artist Maurits Cornelis Escher (Figure 7).

There are a number of patents involving Möbius-type objects, like Möbius conveyor belts and color ribbons that wear evenly on the one-sided surface. Noninductive Möbius

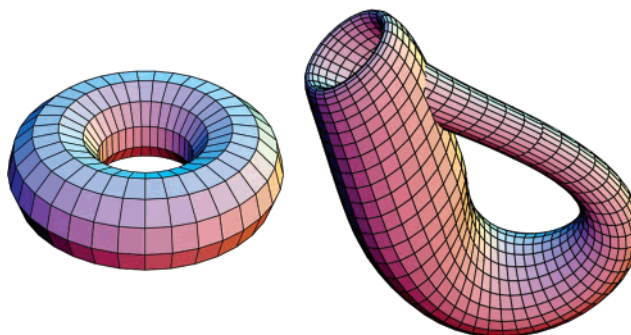


Figure 5. The Klein bottle is a non-orientable surface with no edges. Cut alongside its length two enantiomeric Möbius bands are formed. A torus (orientable) can be cut into a band with an even number of twists (note that only one contiguous cut is allowed).

resistors are used in high-frequency devices.¹¹ The Möbius motif even occurs in literature.⁹ However, Möbius molecules or supramolecular aggregates in nature, to my knowledge, are not known.

2. Non-conjugated Molecular Möbius Strips

In the molecular world, you need either a molecular band with two edges or a π system to define the twisted plane. The first and only synthesis of a molecular band-type Möbius molecule was published by Walba et al. in 1982.^{12,13} They start with a rope-ladder type molecule with ethylene rungs and two polyether ropes. Under high dilution conditions, three different bands are formed: a cylinder, and two enantiomeric Möbius strips.

The symmetry properties of the Möbius molecule are interesting. As static structures the two enantiomers should exhibit C_2 symmetry as shown in Figure 8 (the C_2 axis bisects the crossing of the polyether chains and the double bond on the opposite side of the ring). However, the “twist” that we arbitrarily located exactly between two double bonds can move around the flexible molecule. If the twist is shifted by 60° , into one of the double bonds, a different C_2 conformation is attained. The time-averaged symmetry of all six conceivable C_2 conformations thus is D_6 . Note that D_6 is a chiral point group and the two enantiomers do not interconvert. In typical textbook discussions, chirality is defined by rigidity of the molecular framework (no inversion of the chiral center, no rotation around the chiral axis...), whereas in this case the chirality cannot be located at a center, on an axis, or in a plane, but is a topological property. Topological isomerism¹⁴ (switching between one- and two-sided isomer) might be applicable to the design of quantum computers.¹⁵ The interpretation of the NMR spectra of the Möbius ladder molecule is a challenging exercise in stereochemistry. There is only one sharp ^{13}C NMR signal for all six olefinic carbon atoms, because there are three diastereotopic pairs of homotopic sp^2 carbons (the carbons in each double bond can be matched by a C_2 operation), which are isochronous because they are rapidly interconverted by the fast motion of the twist. The allylic protons are diastereotopic (AB pattern).

Cutting down the middle of an untwisted belt gives two separate rings. The same operation performed on a Möbius band gives one large ring with four half twists. Walba et al. used the ozonolysis reaction to cut the rungs of their molecular ladder and confirmed the above paper strip

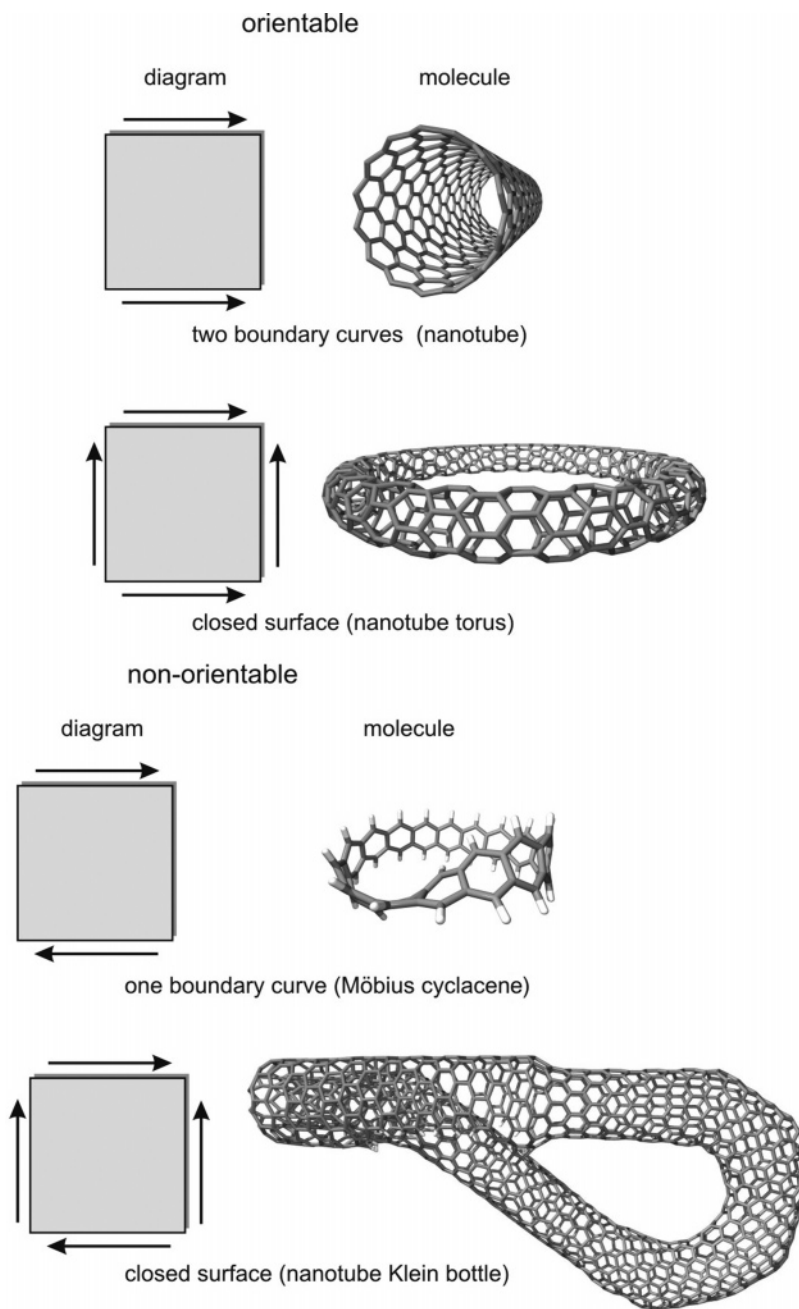


Figure 6. Orientable and non-orientable molecules. The 2D vector diagrams describe a formal procedure to construct objects with the corresponding topology. (The edges of the square have to be brought together in such a way that the arrows match.)

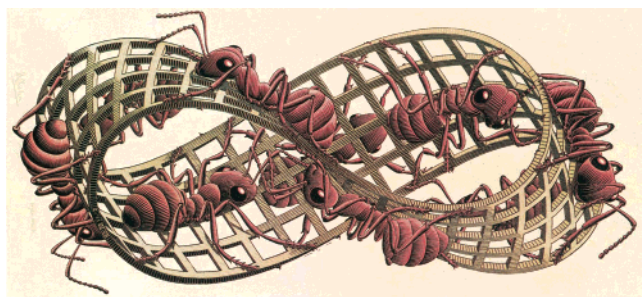


Figure 7. M. C. Escher's "Möbius Strip II".¹⁰ Copyright 2006 The M.C. Escher Company-Holland. All rights reserved. www.mcescher.com.

experiment on the molecular level. The Möbius ladder gave a hexaketone with double the ring size (Figure 9).

Wasserman, who coined the term topological isomerism,¹⁴ proposed an extended rope-ladder type molecule with three

Table 1. Cutting Twisted Bands¹⁶

half twists	cuts	divs. ^a	result
1	1	2	1 band, length 2
1	1	3	1 band, length 2
			1 Möbius strip, length 1
1	2	4	2 bands, length 2
1	2	5	2 bands length 2
			1 Möbius strip, length 1
1	3	6	3 bands, length 2
1	3	7	3 bands, length 2
			1 Möbius strip length 1
2	1	2	2 bands, length 1
2	2	3	3 bands, length 1
2	3	4	4 bands, length 1

^a Number of strips to which the width of the original band is divided.

ropes that would give a catenane with a large ring and a small ring intertwined (Figures 10 and 11).

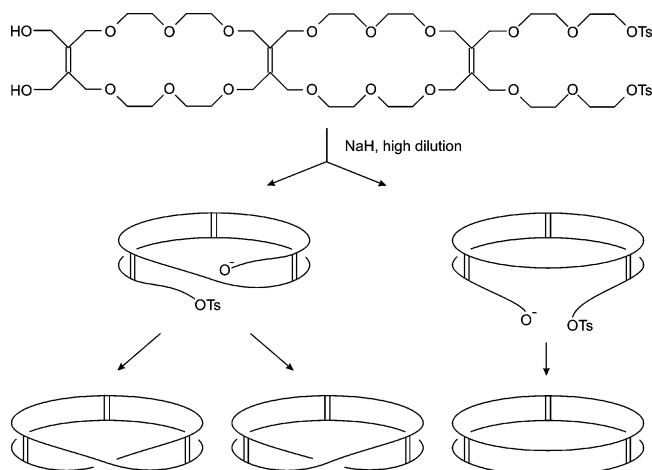


Figure 8. The cyclization of a rope-ladder type precursor yields an untwisted and two enantiomeric Möbius-twisted bands.

An extended list of twisted ring cuttings is given in Table 1.

N. van Gulick published a thorough analysis of the linked ring problem in 1993.¹⁷ H.-W. Xin and W.-Y. Qui in 1997 determined the topological symmetry of the “Möbius ladders” as a function of the number of twists, rungs, and vertices¹⁸ based on the so-called Seifert construction in knot theory.¹⁹

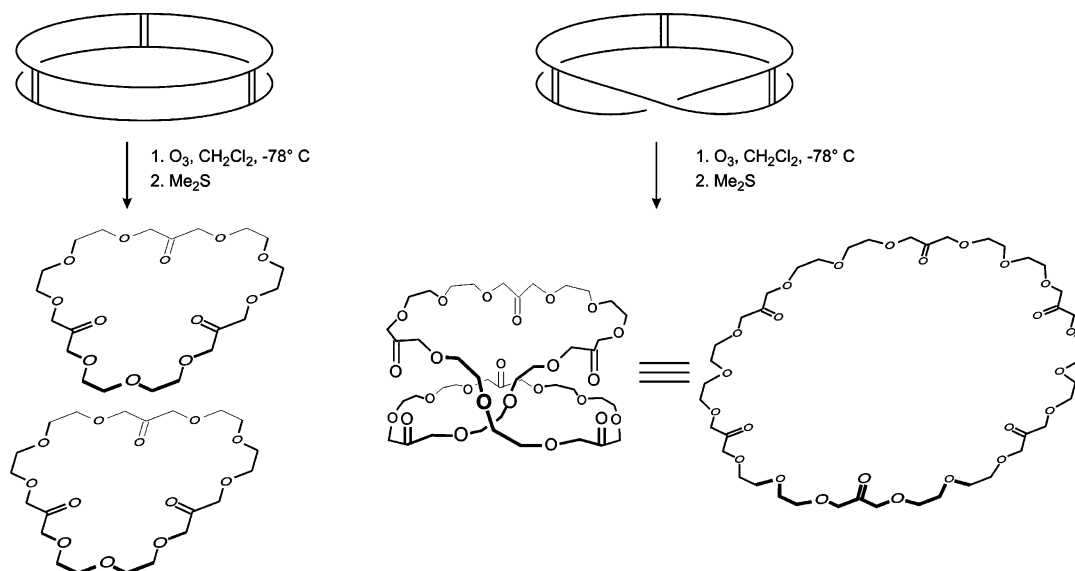


Figure 9. Breaking the rungs (ozonolysis) of the Möbius ladder gives one large ring (hexaketone).

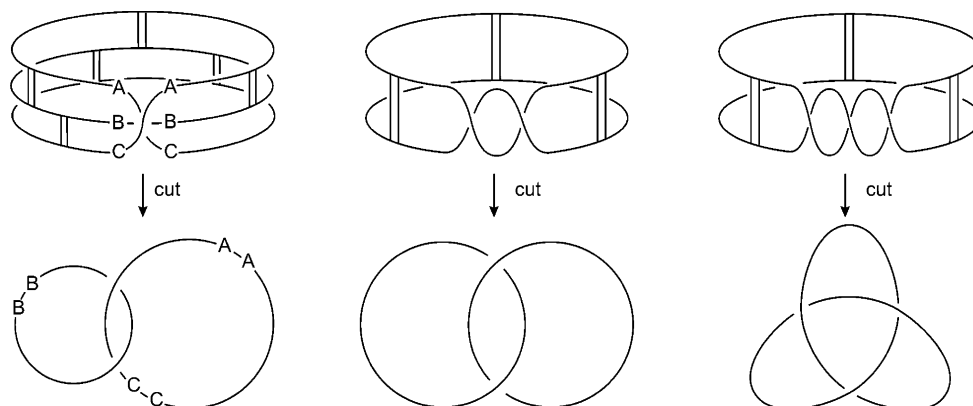


Figure 10. A cyclic rope ladder with three ropes and one Möbius twist cut through all rungs (analogous to the two-rope ladder in Figure 9) gives a catenane with a small and a large ring. A double twisted band cut lengthwise results in two concatenated bands, and a triply twisted band forms a trefoil knot.¹⁷

On the molecular level, these more sophisticated topological operations so far have not been performed, at least not using a rational approach (with the exception of a very funny patent of two school teachers, which was withdrawn shortly after publication).²⁰ However, there is indirect mass spectrometric evidence that complicated “twists and cuts” occur in ring enlargement metathesis reactions (REM) of cyclic olefins. The metathesis reaction of cyclododecene with the WCl₆-EtAlCl₂-EtOH catalyst not only gives the expected higher cyclic polyolefins by repetitive REM, but also catenated rings and probably even trefoil knots and more complicated interlocking rings. The latter are formed by intramolecular REM of twisted precursors (Figure 12).

3. Möbius π Systems

3.1. Theoretical Calculations

3.1.1. Annulenes

In Möbius twisted π systems, the one-sided surface is defined by the nodal plane of the π system. The simplest molecules of this kind are Möbius annulenes. Whereas in a “normal” Hückel annulene all p orbitals can be chosen in such a way that there are only bonding interactions (π molecular orbital of lowest energy), there is at least one sign inversion in the Möbius system as a consequence of the 180°



Figure 11. M. C. Escher's artistic version of a triply twisted Möbius band cut into a trefoil knot. M. C. Escher's "Mobius Strip I".¹⁰ Copyright 2006 The M.C. Escher Company-Holland. All rights reserved. www.mcescher.com.

twist (Figure 13). The analogy with the crab canon of Johann Sebastian Bach (Figure 1) is obvious. In traversing the p-orbital array, the phases of one adjacent pair of orbitals change sign in a manner analogous to the interchange of violin parts in Bach's canon. Both objects, the score of the crab canon (Figure 1) and the Möbius annulene (Figure 13), exhibit the highest symmetry a Möbius object in 3D space can attain: C_2 .

In an idealized planar "equilateral" Möbius band, with an equally distributed twist, the point of sign inversion is not defined. However, real systems such as paper models or molecules always exhibit parts that are more twisted and those that are less twisted. The sign inversion is located in the more twisted part. Similar to a simple paper model, Möbius annulenes are not planar but take the shape of the number 8, when viewed along the C_2 axis, to reduce strain. It should be noted that the σ and the π systems in Möbius annulenes (in contrast to planar annulenes) are not rigorously orthogonal. Particularly in small rings there is considerable σ - π mixing, and therefore considerations based on σ - π separations are crude approximations.

The seminal work on Möbius π systems clearly is Heilbronner's paper on "Hückel molecular orbitals of Möbius-type conformations", which appeared in 1964.²¹ On the basis of simple HMO theory,^{22,23} he predicted that the Hückel rules for aromaticity ($4n+2$ electrons) are no longer valid for Möbius twisted annulenes. He assumed an equally distributed twist around the (equilateral) Möbius ring. As a consequence, the overlap of neighboring p orbitals is reduced

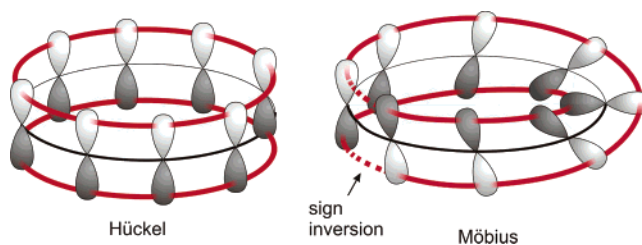


Figure 13. A Hückel and an idealized equilateral (planar) Möbius annulene. The π overlap is indicated in red. The π plane in the Hückel annulene has two sides, and there are two separate " π clouds", above and below the ring plane (two red circles). However, there is only one side in the π system of the Möbius annulene (one closed red curve). As a result of the twist, there is (at least) one sign inversion (dotted lines) between neighboring p orbitals. Note the analogy with the crab canon of J. S. Bach (Figure 1). The two phases of the p orbitals change sign in a similar way as the two violins in Bach's canon in the middle of the score.

and the resonance integral β should be replaced by $\beta \cdot \cos(\pi/N)$ (N = number of ring atoms). Another ramification of the twist is a sign inversion (an antibonding orbital overlap) at some point, which is accounted for as $-\beta$ for one of the resonance integrals in the secular equation. Heilbronner included both boundary conditions and obtained a closed analytical solution for the secular equation similar to the solution for the "normal" Hückel annulenes. Comparing both π energies for a Hückel and a Möbius annulene of the same size, Heilbronner concluded that: "... a planar perimeter of $4n$ AO's, which would yield an open shell configuration when occupied by $4n$ electrons, can be twisted into a closed shell Möbius strip perimeter without loss in π electron energy." In other words, if you start with an antiaromatic $[4n]$ annulene, cut one of the bonds, twist the linear p system by 180° , and close the ring again, the π energy should remain the same. Heilbronner also predicted that larger annulenes (ring size >20) should tolerate a twist without any apparent strain. This is a very cautiously formulated statement that large Möbius annulenes should be stable molecules.

Zimmerman in 1966 introduced a mnemonic device to memorize the π orbital energies of Möbius annulenes,²⁴ which is similar to the Frost-Musulin mnemonic for Hückel systems (Figure 14).²⁵

In the Frost-Musulin diagram, the n -gon representing the $[n]$ annulene is inscribed in a circle with the diameter of 4β with a center at an energy of α (the Coulomb integral α and

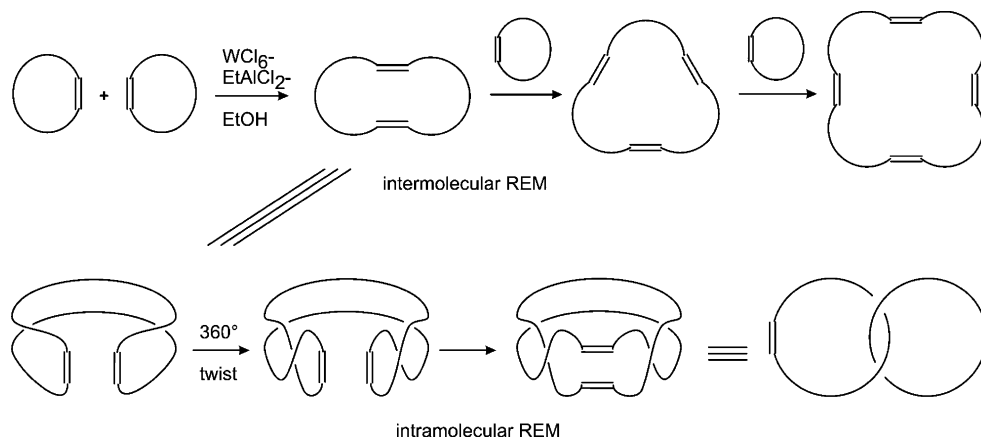


Figure 12. Cyclododecene undergoes two types of transition metal-catalyzed ring enlargement reactions (REM). The intermolecular reaction gives (as expected) higher cyclic polyolefins. With a large enough ring size, these cyclic polyolefins undergo intramolecular REM. The REM of an untwisted ring conformation yields two smaller rings. A 180° Möbius twist gives rise to one ring of the same size, a 360° twisted conformation forms two interlocked rings (bottom), and 540° (triple Möbius twist) gives a trefoil knot (not shown).¹⁷





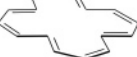
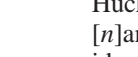



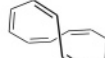
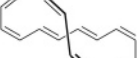
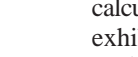
[<i>n</i>]annulenes	<i>n</i> =6	<i>n</i> =8	<i>n</i> =12	<i>n</i> =16	<i>n</i> =20
					
					
ΔE [kcal/mol]	107.0	21.3	6.3	5.2	6.3

Figure 16. Relative energies of the most stable Hückel and the most stable Möbius isomer of [6]-, [8]-, [12]-, [16]-, [20]annulene, calculated at the B3LYP/6-31G* level of DFT.

trans bond. Hypothetical *trans*-benzene (C_2) is predicted to be extremely strained and only a shallow minimum on the energy hypersurface ~ 100 kcal mol $^{-1}$ higher in energy than D_{6h} benzene (calculated at several levels of theory).^{27–29} The energy difference between *all-cis*- and *trans*-cyclooctatetraene according to DFT calculations is about 21 kcal mol $^{-1}$.²⁷ Obviously, the increase in ring size compensates for part of the strain imposed by the trans bond as compared to the *trans*-benzene. Neither *trans*-benzene nor *trans*-cyclooctatetraene are aromatic according to the magnetic criteria (NICS = -1.7 and -1.9). The conjugation between the trans and the neighboring cis double bonds is reduced by dihedral angles, which are close to 90° . As expected, the energy difference between the most stable Hückel and Möbius isomer is further reduced in the [12]- and [16]annulene manifold (Figure 16).^{30,31} However, in the set of the [20]-annulenes, the energy difference with 6.3 kcal mol $^{-1}$ increases again.

Obviously, any stabilization by Möbius aromaticity cannot overcome the destabilization induced by strain or the reduced overlap of neighboring p orbitals. Ab initio and DFT calcula-

tions, in agreement with experimental data, predict that the most stable isomer of each [4*n*]annulene, up to $n = 5$, has Hückel topology! Crystal structures that are available for the [*n*]annulenes ($n = 6, 8, 14, 16, 18$)^{32–34} and all structures identified by NMR or a combination of NMR and theoretical calculations (KMLYP functional of density functional theory)²⁶ exhibit Hückel topology. There is no experimental data available for any neutral, parent Möbius annulene.

Both Heilbronner²¹ and Zimmerman²⁴ were reluctant to use the term “aromatic” to characterize Möbius annulenes or Möbius transition states. However, according to the calculations of Castro et al.,³⁰ some of the twisted isomers of the [12]-, [16]-, and [20]annulenes clearly are aromatic. They exhibit strongly negative NICS values (strong NMR upfield shift of a hypothetical atom in the center of the ring)³⁵ and a pronounced bond length equalization. The NICS value, -14.5 , of the Möbius [16]annulene (Figure 17) is of similar size to the NICS of benzene (-11.5). The C–C bond lengths do not systematically alternate and are close to the value in benzene (the longest is 1.411 Å and the shortest 1.392 Å). As expected, the twist is not equally distributed; however, with 29.1° the largest deviation from planarity is quite small, and thus the conjugation is not interrupted.

There are 2250 conceivable cis/trans isomers of [16]-annulenes, many of which are not stable because they are highly strained. In a more systematic theoretical study, we determined the 153 most stable isomers of [16]annulene and analyzed their aromatic properties. There is a continuum between truly aromatic, twisted Möbius isomers, nonaromatic rings with dihedral angles close to 90° , and antiaromatic Hückel structures.

In Figure 18, two different aromaticity parameters of the [16]annulene isomers are plotted as a function of each other. The NICS values (*x*-axis) vary between $+19.3$ (very antiaromatic) and -14.5 (strongly aromatic). The HOMA values

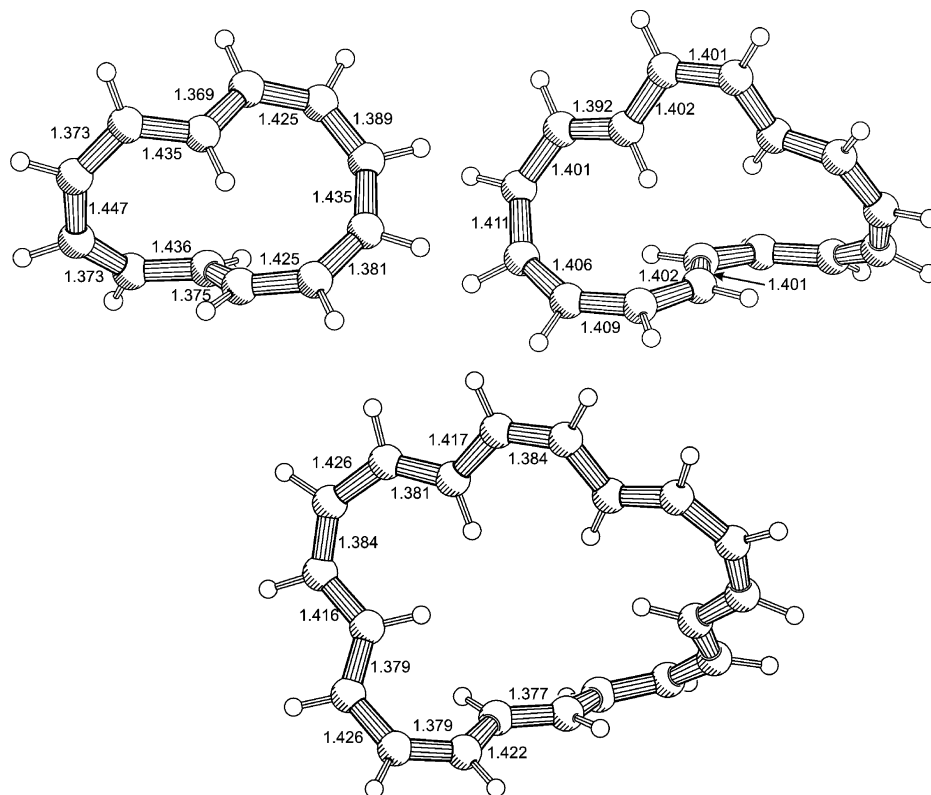


Figure 17. Theoretically calculated structures (B3LYP/6-31G*) of the hypothetical “most aromatic” Möbius [12]-, [16]-, and [20]-annulenes.³⁰

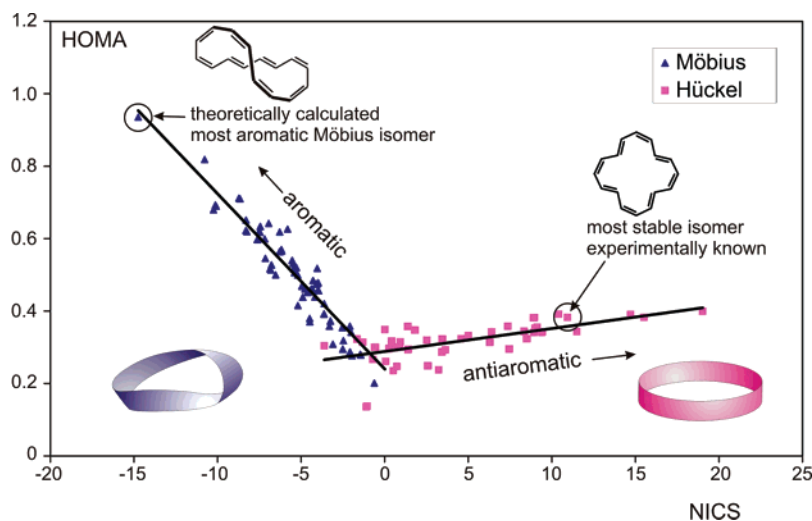


Figure 18. Aromaticity of the 153 most stable isomers of [16]annulene. Two different aromaticity measures, the NICS value (GIAO, B3LYP/6-31G*) and HOMA (a quantitative measure of the bond length equalization), are plotted as a function of each other. Möbius isomers are marked with blue triangles and Hückel structures with pink squares. Aromatic molecules exhibit negative NICS values and large HOMA values.

(y-axis), which are a quantitative measure of bond length equalization³⁶ (HOMA of benzene = 1.0), also range from 0.135 (weakly conjugated) to 0.935 (almost perfect bond length equalization). Interestingly, there is no correlation between the energy and aromaticity. The experimentally known compound of which two X-ray structures are published^{37,38} is rather antiaromatic. This is in agreement with the large upfield shift of the ¹H NMR signals of the inner hydrogen atoms of 10.4 ppm.³⁹ Obviously, the energies of the annulene isomers are dominated by strain energy and not by any aromaticity stabilization. For the Möbius isomers, the correlation between NICS and HOMA is excellent. As expected, isomers with negative NICS exhibit a large HOMA. However, an NICS versus HOMA plot for Hückel structures shows the opposite correlation. Isomers that exhibit a stronger bond length equalization (more effective conjugation) have a stronger paratropic ring current and thus more antiaromatic magnetic properties. Isomers in the vicinity of the intersection point of the two lines are nonaromatic. They exhibit dihedral angles close to 90° and thus an interrupted conjugation. Summing up, neutral [4*n*]annulenes that traditionally would be classified as Hückel antiaromatic, in principle, can be truly aromatic if they exhibit a 180° Möbius twist. A precondition for a strong aromaticity is that the twist is well distributed over the ring, keeping the dihedral angles close to 0° (cis) or 180° (trans).

The unusual ring currents in Möbius annulenes are particularly interesting. In “normal” aromatic annulenes, there is a strong ring current induced by an external magnetic field perpendicular to the ring plane. The current is clockwise if the magnetic field vector points toward the viewer. The magnetic field induced by the ring current is opposed to the external field inside the ring and parallel on the outside, giving rise to an upfield NMR shift of protons in the ring and a downfield shift of the “outer” protons. Antiaromatic annulenes exhibit exactly the reverse characteristics, an anticlockwise ring current, a downfield shift inside, and an upfield shift outside the ring. In the prototypical aromatic system, benzene, the magnetic properties are surprisingly accurately predicted by reducing the π system to the classical system of two conducting wires above and below the ring (see red circles in Figure 13, Hückel). If we stick to the simple wire model, the current in a Möbius annulene must

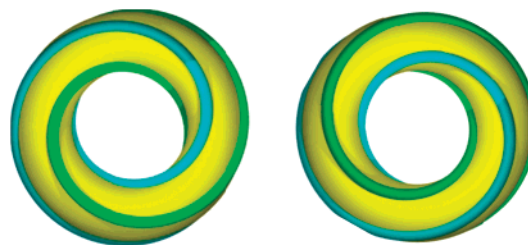


Figure 19. Clockwise and anticlockwise “winding” ring currents in two idealized, equilateral, enantiomeric Möbius systems.

“wind” around the ring (red curve in Figure 13, Möbius). The rotational direction of the “winding” in Möbius structures is clockwise in one and anticlockwise in the other enantiomer (Figure 19).

“Real” Möbius molecules are not planar, and there is no unambiguous relative orientation of the magnetic field and the molecule. Most of the Möbius isomers that we located using DFT calculations have the shape of the number 8 and exact or at least approximate C_2 symmetry (like the simple paper model of a Möbius strip). So one might ask what the relative orientation of the molecule and the magnetic field should be, to induce a maximum ring current. A “figure eight”-shaped, D_2 symmetric 3D object (closed curve, no intersection) has three symmetric projections along all three C_2 axes (Figure 20).

A magnetic field orthogonal to the projection plane would not induce any ring current in the orientations (a) and (b). The ring currents in both loops of the “eight”-shaped projection cancel each other. Projection (c) corresponds to a closed curve with no intersection and gives rise to a ring current.

In Figure 21, the orientation of the magnetic field relative to the C_2 symmetric Möbius [16]annulene is chosen in such a way that a maximum ring current is induced (projection (c), Figure 20). The ACID scalar field^{40,41} (anisotropy of the induced current density, yellow isosurface), which represents the density of delocalized electrons, indicates that there is a continuous cyclic conjugation. The current density vectors (green arrows on the ACID isosurface) indicate a diatropic ring current, and they make a half-twist around the small diameter of the deformed torus.

Whereas the experimentally known neutral [4*n*]annulenes all exhibit Hückel topology, the most stable isomer of the

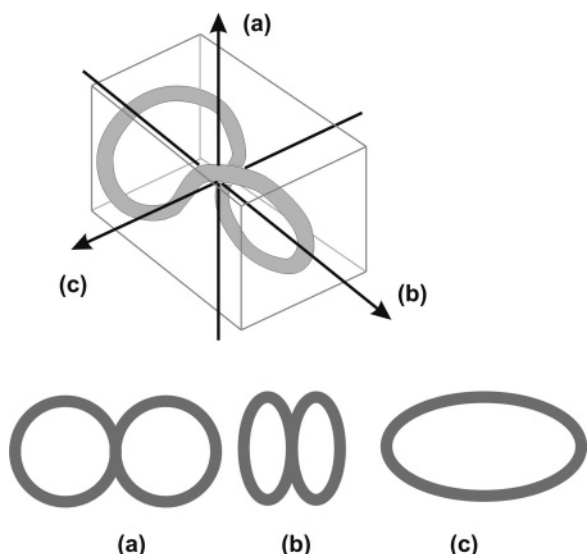


Figure 20. There are three symmetric projections of a “figure eight”-shaped, D_2 symmetric object onto a plane. If a magnetic field were applied perpendicular to the projection plane, only orientation (c) would give rise to a ring current.

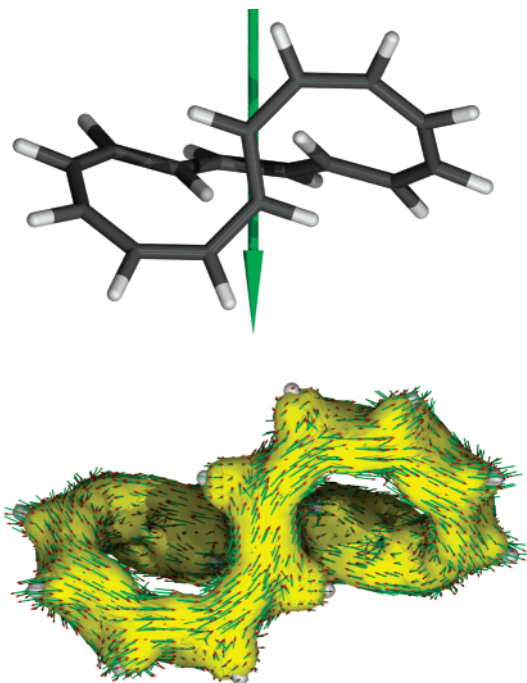


Figure 21. Ring current in the C_2 symmetric Möbius¹⁶ annulene. The current density vectors (green arrows) are drawn on the ACID isosurface (yellow, isosurface value 0.05). The orientation of the magnetic field is indicated by the large green arrow.

[9]annulene cations probably is a Möbius ring. In the early 1960s, the thermal rearrangement of 9-chlorobicyclo[6.1.0]-nonatriene to 1-chloro-8,9-dihydroindene was observed.⁴² LaLancette and Benson suggested a chlorocyclononatetraene as the intermediate.⁴³ In 1971, Schleyer and Boche discovered that the trans configuration of 9-chlorobicyclo[6.1.0]-nonatriene labeled with deuterium in the 9-position upon solvolysis gives a dihydroindene product with D completely scrambled to all positions and suggested a cyclononatetraenyl cation as the intermediate (Figure 22).⁴⁴ Yakali in her dissertation (1973) was the first to suggest that this cation could have a Möbius twisted structure.⁴⁵ She suggested a “coiled carbonium ion”, which would rapidly automerize via a planar transition state.^{46,47}

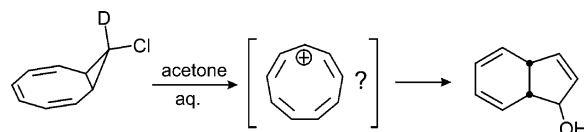


Figure 22. The solvolysis of 9-deutero-9'-chlorobicyclo[6.1.0]-nonatriene proceeds via a cyclononatetraenyl cation intermediate and yields a dihydroindene with the deuterium scrambled over all ring positions.⁴⁴

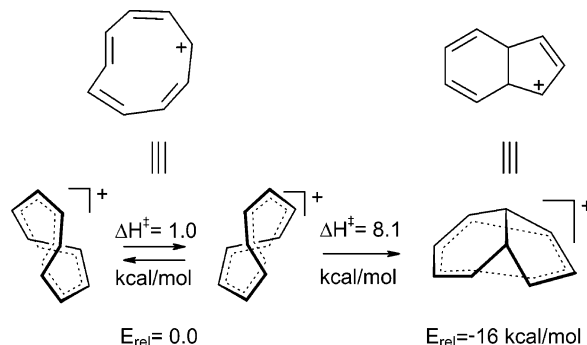


Figure 23. DFT calculations confirm that the short-lived intermediate in the rearrangement of 9-chlorobicyclo[6.1.0]nonatriene is a Möbius [9]annulene.

Schleyer et al., using DFT calculations, provided convincing evidence that the [9]annulene cation indeed has Möbius topology and C_2 symmetry (Figure 23).⁴⁸ The barrier for racemization is only about 1 kcal mol⁻¹. An electrocyclic ring closure with a barrier of 8.1 kcal mol⁻¹ leads to a bishomo-aromatic bicyclic product, which is 16 kcal mol⁻¹ more stable than the [9]annulene cation. The low activation barrier and the stability of the product are in agreement with the short half-life of the intermediate of only 10 min at -66 °C in liquid SO₂. A direct structural proof, however, has not been provided.

3.1.2. Cyclacenes

Cyclacenes have been theoretically investigated^{49–52} and proposed as interesting synthetic targets. Polyacenes are increasingly unstable as the number of benzene rings increases.^{53–57} Despite repeated attempts, no cyclacenes have been prepared.^{58–63} The prospects for a successful synthesis of a strained Möbius cyclacene are not good. Nevertheless, in view of their peculiar electronic structures, Möbius π systems are worthy of investigation.

Mizoguchi in 1989⁴⁹ and André et al.⁵² in 2001 presented analytical solutions of the HMO-ansatz for polyacenes, cyclacenes, and Möbius cyclacenes. Polyacenes behave very much like the corresponding annulenes. The transannular bonds only have a moderate effect on the electronic structure. The HOMO–LUMO gap (and the λ_{\max} of the UV/vis absorption) is a linear function of the size of the π system, monotonically decreasing with the number of benzene rings. The non-twisted cyclacenes exhibit an unusual behavior. If they include an even number of fused benzene rings, HMO theory predicts a degenerate HOMO and LUMO, and those with an even number of benzene rings have a distinct HOMO–LUMO gap, which decreases with increasing size of the π system. The result is a “sawtooth-like” conductor/semiconductor alternation of the gap.⁵² Möbius cyclacenes, like the polyacenes, again exhibit a monotonically decreasing HOMO–LUMO gap with increasing ring size. These results can be easily rationalized by removing the transannular bonds of the cyclacenes. By “breaking the rungs of the ladder” (see also Figure 9), the electronic structure is not dramatically

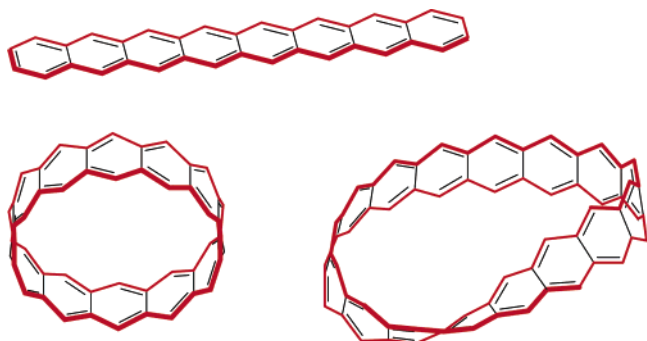


Figure 24. A polyacene, cyclacene, and Möbius cyclacene. The polyene periphery is depicted in red.

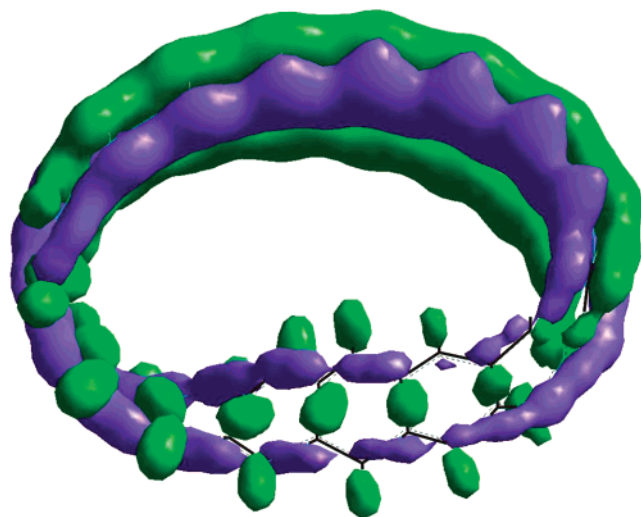


Figure 25. The lowest lying “ π -type” molecular orbital of the Möbius [16]cyclacene exhibits considerable σ (C–C and C–H) contribution in the vicinity of the twist (AM1).

perturbed. In the non-twisted cyclacene (or cyclacenes with an even number of twists), there are two independent annulene rings left (red lines in Figure 24). The annulene periphery is simply aromatic with $4n+2$ electrons if the cyclacene includes an odd number of benzene rings and antiaromatic if the cyclacene contains an even number of benzene rings ($4n$ electrons) (suggesting the synthesis of an odd membered cyclacene instead of the [12]- and [8]-cyclacene attempted by Stoddart and Corey).^{59–63} A Möbius band, however, has only one edge and thus only one annulene periphery of double the size as the corresponding untwisted band (see red curve in Figure 24). Therefore, this “coiled” annulene always includes $4n$ electrons irrespective of the number of benzene rings included in the Möbius cyclacene. The simple HMO predictions qualitatively hold at a semiempirical level of theory.^{50,51} Rzepa calculated the structure of several Möbius cyclacenes and observed as a common feature of all geometries that the twist is not evenly distributed around the ring but localized to a few benzene rings.⁵¹ Consequently, the HOMO and the LUMO have small coefficients in the region of the twist. Lower lying π orbitals exhibit an increasing contribution by the σ system. This is to be expected because the π and the σ systems are not strictly orthogonal in nonplanar structures (Figure 25).

3.1.3. Kekulene and Other Coronoid Structures

Synthetically more promising targets as compared to the Möbius cyclacenes are those polycyclic aromatic hydrocarbon (PAH) structures that are not linearly fused. However,

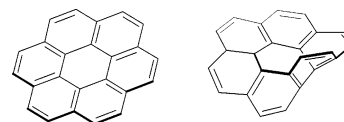


Figure 26. Coronene and Möbius coronene.

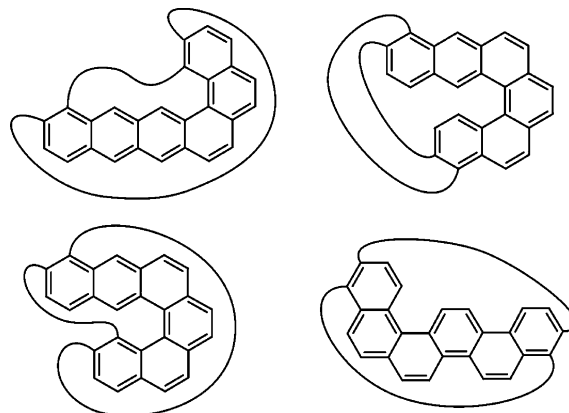


Figure 27. Four isomers of coronene of which the Möbius structure is more stable than the non-twisted Hückel topological isomer. The curved lines indicate the position of ring fusion.

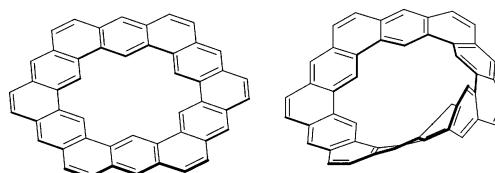


Figure 28. D_{6h} symmetric planar kekulene and the most stable (C_2 symmetric) Möbius kekulene.

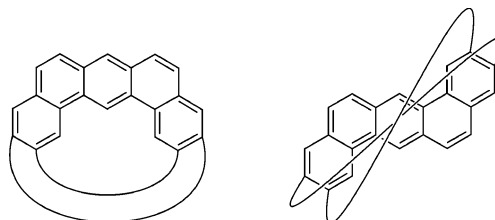


Figure 29. Simplified view of the planar and the Möbius kekulene structure. The curved lines are an abbreviation of the remaining seven benzene rings.

in contrast to the cyclacenes, there are more isomers and more than one way to introduce the twist into the same structure. Therefore, the stereochemistry is more complex. The smallest conceivable Möbius coronoid system is Möbius coronene.⁶⁴ Dobrowolski systematically investigated about 100 constitutional unbranched cyclic catacondensed isomers of coronene and optimized the structures using semiempirical and ab initio methods.⁶⁵ The most stable isomer with no twist of course is coronene. Twisted Möbius coronene (Figure 26) is about $200 \text{ kcal mol}^{-1}$ less stable and probably beyond the reach of any synthetic attempt.

However, among the isomers listed by Dobrowolski there are four Möbius structures, which are more stable than their Hückel topological isomers (Figure 27).

Among the plethora of PAH's that are formed by high-temperature coking of coal, there might be one of these Möbius structures.⁶⁵

Larger coronoids are able to accommodate the strain induced by the twist more easily. Planar D_{6h} kekulene, which consists of 12 cyclic annelated benzene rings, was synthe-

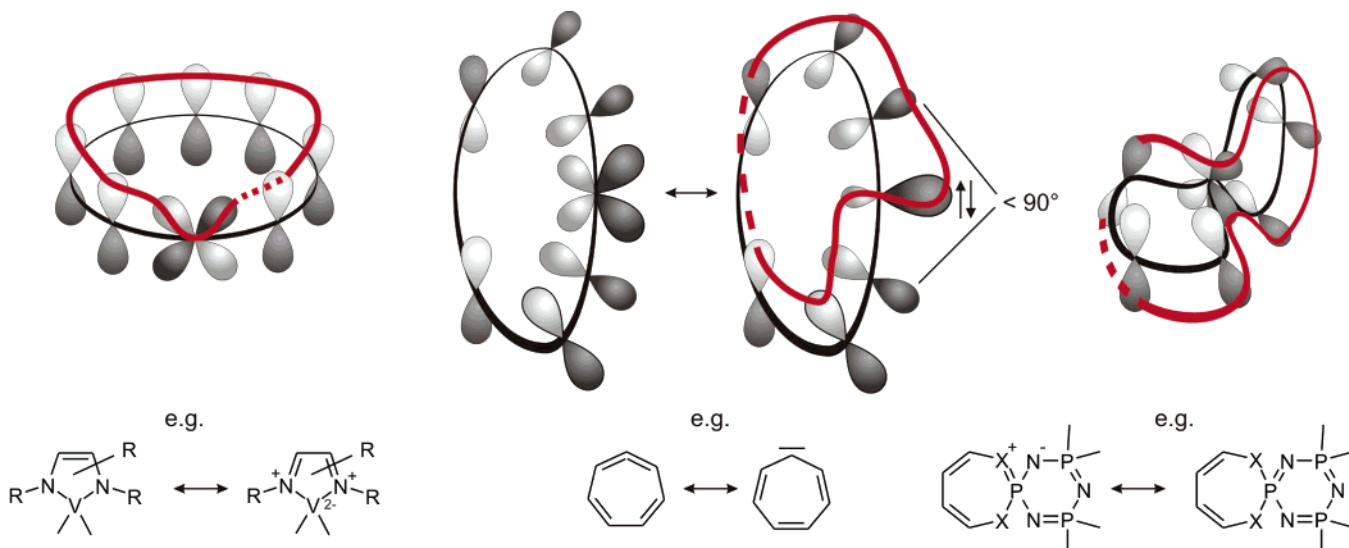


Figure 30. Möbius systems, proposed by Rzepa.⁷⁰ Left, “Craig^{68,69}-type system” using a d orbital to introduce a sign inversion; middle, allene unit in a strained ring; right, “coarctate”⁷⁴ spiro system. The orbital drawings all include eight basis orbitals. The topology of the orbital overlap is indicated by a red curve. Sign inversions are depicted as dashed lines. Note that a red line passing the origin of a basis orbital does not define a sign inversion (only the overlap of two different basis orbitals with different phase causes a sign inversion).

sized by Staab and Diederich in 1978 (Figure 28).^{66,67} Zoellner et al. systematically investigated twisted kekulenes.⁶⁴ There are four different ways to introduce the twist. According to our calculations (PM3), the four isomers rapidly interconvert and two of them are considerably more strained than the other pair. The most stable Möbius isomer is only 56 kcal mol⁻¹ less stable than the planar kekulene.

Thus, a synthesis is not completely unrealistic. For designing a synthetic approach, it is instructive to draw the structure in a simplified way and from another viewpoint as depicted in Figure 29.

Unlike the synthesis of the planar kekulene,⁶⁷ the synthesis of the Möbius topological isomer should start with an S- instead of a U-shaped tetrahydrodibenzoanthracene unit.

3.1.4. Other Möbius Systems

In a series of articles, Rzepa proposed “electronic” ways to introduce a sign inversion into cyclic conjugated structures: (a) introducing d orbitals,^{68–70} (b) allene units,^{71,72} or (c) a coarctation in spiroaromatic systems⁷³ (Figures 30 and 31). These Möbius systems have been thoroughly reviewed by Rzepa⁷⁰ and therefore will only be briefly discussed here. Craig was the first to propose that a d orbital should induce a phase inversion in a π system.^{68,69} In an annulene, this should have the same effect as a 180° twist. Allenes included in an annulene induce a 90° twist and would shut off conjugation. In strained medium-sized rings, however, the orthogonality is broken (e.g., ~50° dihedral angle in cycloheptatetraene), and the allene building block can be used to induce a twist. In spiro systems, the spiro atom can provide two p orbitals for delocalization, and like the coarctation^{74–82} this may induce an electronic Möbius topology.

Recently, Fowler proposed that cyclopropane can be viewed as being Möbius aromatic.⁸³ The in-plane tangential p orbitals may be used to construct delocalized molecular orbitals similar to out-of-plane π orbitals using the Frost–Musulin–Zimmerman mnemonic (Figure 31). There is a sign inversion and thus a Möbius topology in odd membered rings even though they are untwisted. Cyclobutane with no sign inversion and four tangential orbitals would be Hückel antiaromatic.

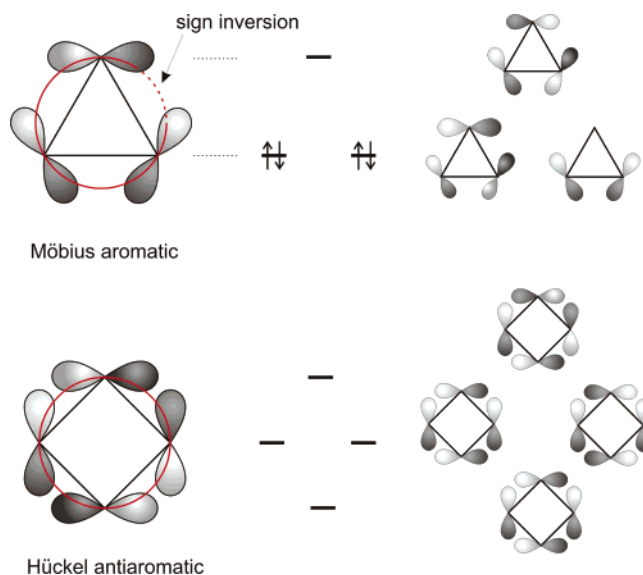


Figure 31. In-plane Möbius aromaticity in cyclopropane and in-plane antiaromaticity in cyclobutane.

ACID calculations are in agreement with this qualitative concept for cyclopropane and cyclobutane (Figure 32). There is a strong conjugation and a diatropic ring current mainly in the outer periphery (tangential orbitals) in cyclopropane and a paratropic ring current in cyclobutane.

The paratropic ring current gives rise to an abnormally high magnetic susceptibility and a strongly negative NICS value (−42.8 ppm) in cyclopropane, and the paratropic current leads to a low magnetic susceptibility and a positive NICS (+2.6 ppm) in cyclobutane.^{84,85}

3.1.5. Möbius Transition States

Möbius transition states have been proposed by Zimmerman²⁴ only 2 years after Heilbronner’s seminal paper on Möbius annulenes (Figure 33). Zimmerman’s Hückel/Möbius method⁸⁶ and Dewar’s closely related aromaticity concept⁸⁷ for predicting the stereochemistry of pericyclic reactions are alternatives to the Woodward–Hoffmann rules⁸⁸ and found reception in many textbooks of mechanistic organic chem-

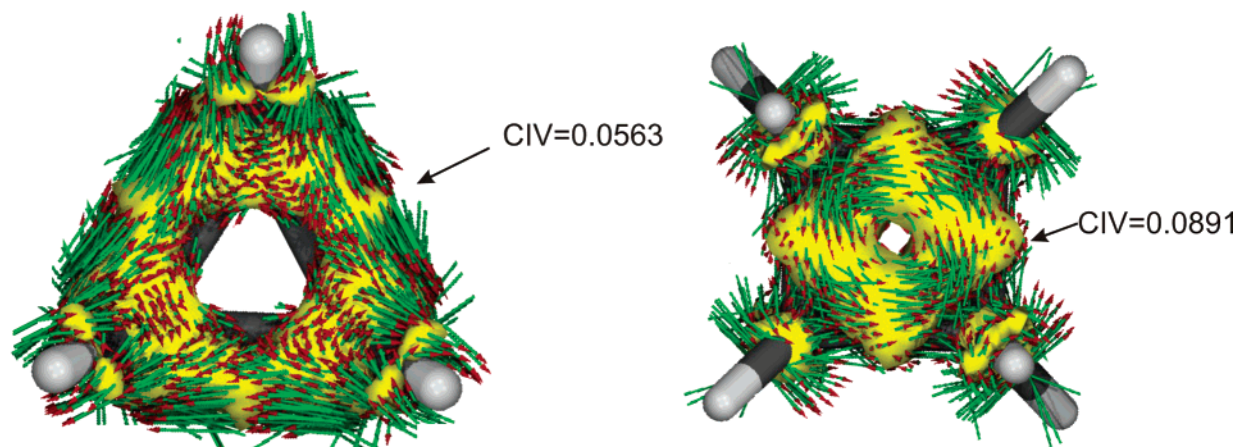


Figure 32. ACID plot of cyclopropane and cyclobutane (B3LYP/6-31G*, isosurface value = 0.05). Current density vectors are plotted onto the isosurface (magnetic field orthogonal to the ring plane and pointing to the viewer). There is a strong diatropic ring current in cyclopropane (clockwise, Möbius aromatic) and a paratropic ring current in cyclobutane (anticlockwise, Hückel antiaromatic).

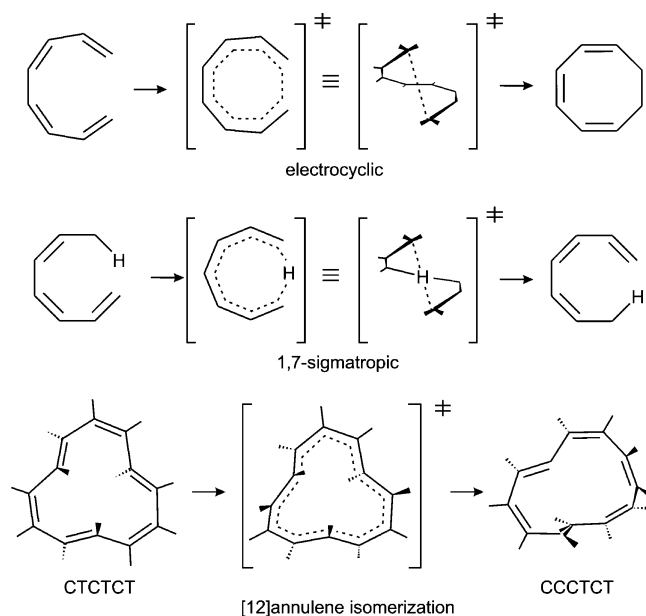


Figure 33. Möbius transition states. Top, conrotatory electrocyclic ring closure of (*Z,Z*)-octa-1,3,5,7-tetraene to (*Z,Z,Z*)-cycloocta-1,3,5-triene; middle, antarafacial, automeric 1,7-sigmatropic shift of (*Z,Z*)-hepta-1,3,5-triene; bottom, isomerization of the most stable [12]-annulene to a less stable (*Z,Z,Z,E,Z,E*) isomer.

istry. It is probably still the most important practical application of Heilbronner's idea of Möbius twisted π systems. Hückel and Möbius transition states of pericyclic reactions exhibit magnetic properties that are in the range of aromatic compounds and classify them as truly aromatic.^{89,90} Castro and Karney recently proposed a Möbius aromatic transition state in the isomerization of (*Z,E,Z,E,Z,E*)-¹²annulene (most stable (CH)₁₂ isomer) to (*Z,Z,Z,E,Z,E*)-¹²annulene (Figure 1).⁹¹

3.2. Design and Synthesis of the First Möbius Annulene

Numerous attempts notwithstanding, since Heilbronner's theoretical prediction in 1964, it took almost 40 years to synthesize the first stable Möbius twisted π system.^{92,93} The main problem in preparing a Möbius annulene is the fact that all parent annulenes with a ring size of 4–20 (and most probably also the larger ones) are more stable in a non-

twisted topology. As outlined in section 3.1.1 (and depicted in Figure 16), the stabilization of the π system in [4*n*]-annulenes by Möbius aromaticity cannot overcome the strain induced by the 180° twist. There are Möbius isomers among the [8]-, [12]-, [16]-, and [20]-annulenes; however, they are higher in energy and kinetically unstable. The extensively investigated energy hypersurface of the parent [16]annulene exemplifies the problem. Both the Schröder/Oth and the Sondheimer/Gaoni reactions give the most stable [16]-annulene (*S*₄ symmetric) isomer, which in solution is in equilibrium with a lower concentration of the second most stable isomer.^{94,95} The coalescence temperature of isomerization in the ¹H NMR spectrum is –57 °C. Moreover, each of the two isomers is in equilibrium with 8 or 32 symmetry equivalent isomers, which are formed by *cis/trans* isomerization or double bond shift. The automerizations are rapid at the NMR time scale even at temperatures lower than –100 °C (Figure 34).^{39,96}

The [16]annulene isomer with the strongest Möbius aromaticity predicted so far is 15.8 kcal mol^{–1} higher in energy than the global minimum and number 137 in the list of the most stable isomers. There is probably no chance to prepare such a species even at low temperatures. The larger annulenes, for example, the [20]annulene, are even more flexible structures.

To obtain a stable Möbius annulene, the twist has to be stabilized by proper substitution or incorporation into a rigid molecular frame. To develop a strategy, it is instructive to examine the π system of Möbius annulenes in more detail. There are two types of cyclic π conjugation: (a) the “normal” (anti)aromatics with the p orbitals perpendicular to the ring plane and (b) “in-plane” (belt-like) conjugated systems in which the inner lobes of the p orbitals all point toward the axis of the belt or tube (Figure 35). In “normal” aromatics, the sp²-hybridized ring atoms retain their preferred trigonal planar configuration, whereas “in-plane” conjugated systems exhibit pyramidalized sp² centers (with partial sp³ character). In rings with a not very large diameter, pyramidalization causes a considerable amount of strain. Therefore, these compounds are much less common than “normal” aromatics and usually have a large diameter (e.g., carbon nanotubes). Möbius annulenes exhibit both types of aromaticity: “normal” and “in-plane”.

The strain arises mainly from the pyramidalized part. A suitable strategy stabilizing the pyramidalized “in-plane” part

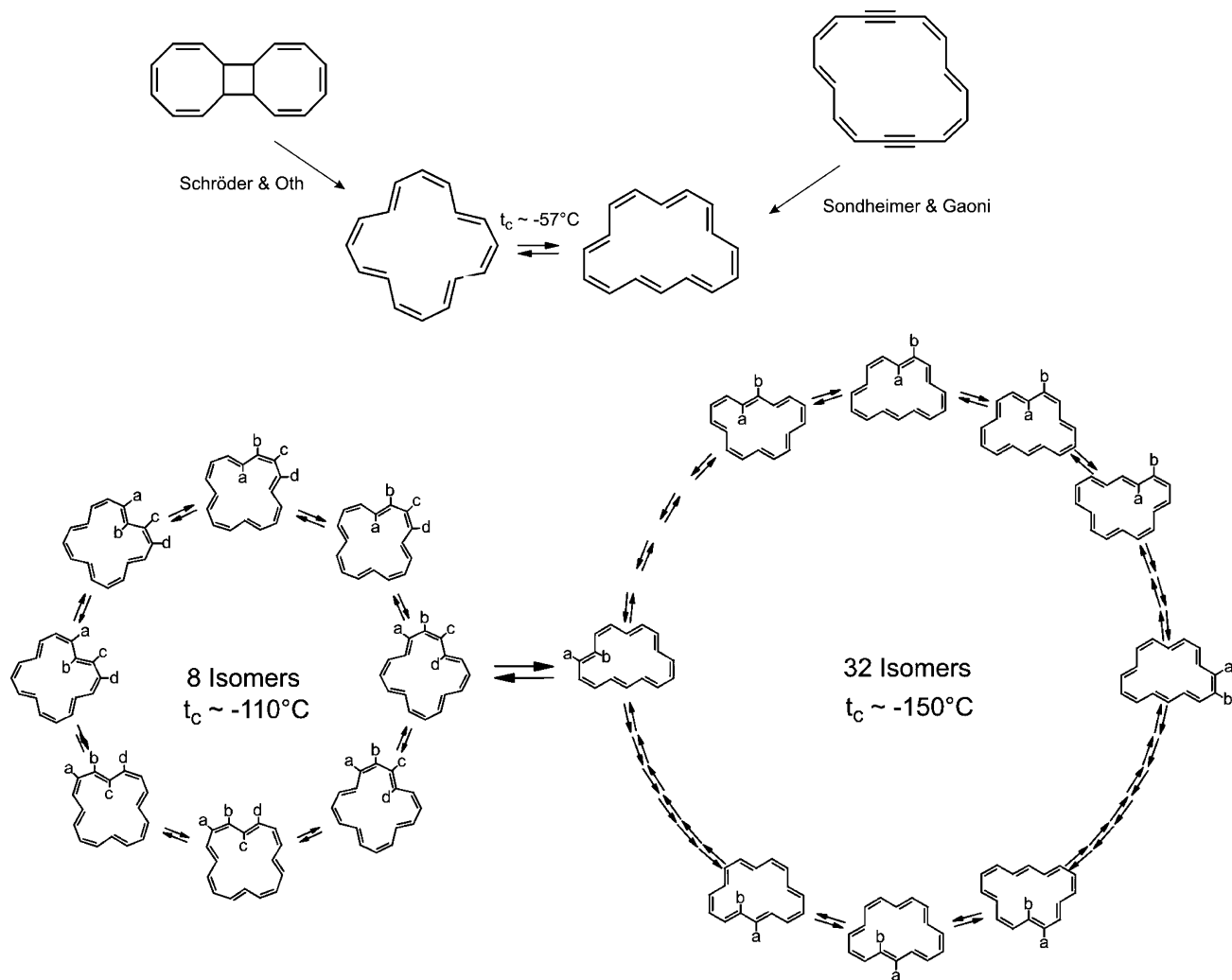


Figure 34. The parent [16]annulene is conformationally and configurationally extremely flexible.

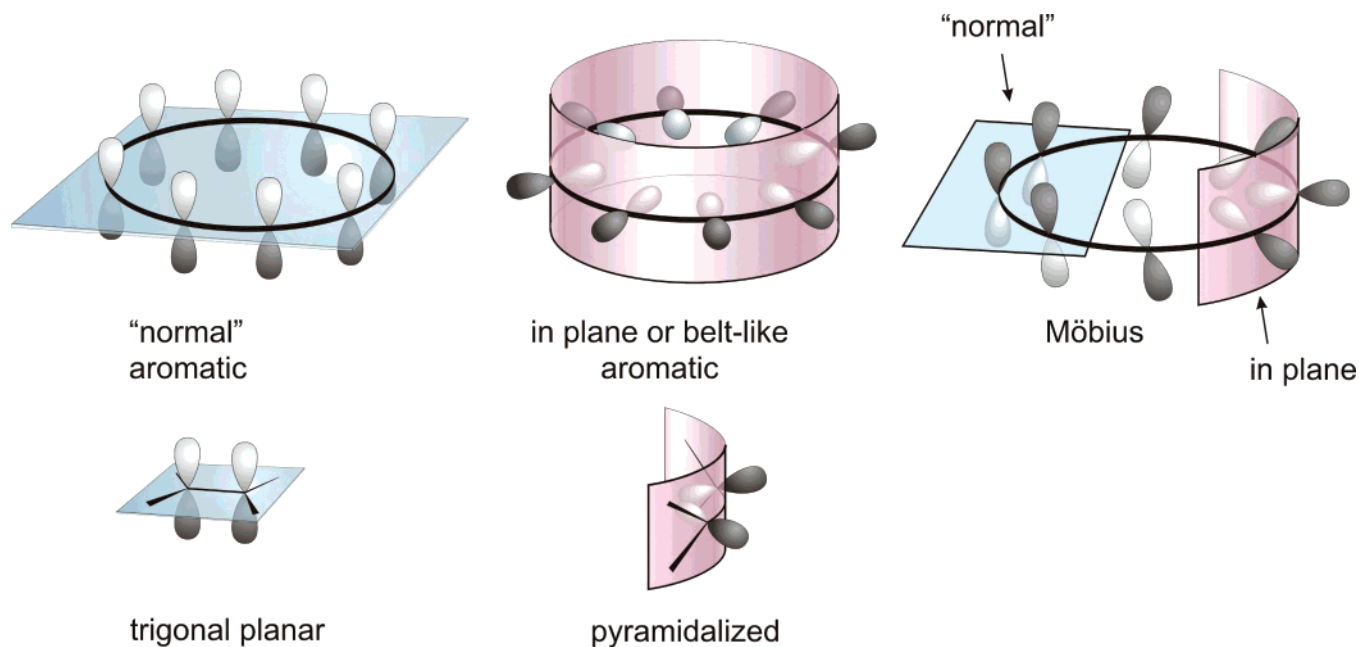


Figure 35. Möbius annulenes include a “normal” (cyan) and an “in-plane” (magenta) conjugated part. The strain in Möbius annulenes is mainly localized in the “in-plane” part in which the sp^2 -hybridized atoms are pyramidalized.

of the annulene should also stabilize the twist. Most of the experimentally known pyramidalized double bonds are included in a polycyclic ring system, distorting the trigonal

sp^2 carbon atoms out of plane.⁹⁷ However, the convex side of the pyramidalized double bond is now blocked to further substitution (Figure 36a). Therefore, a strategy relying on

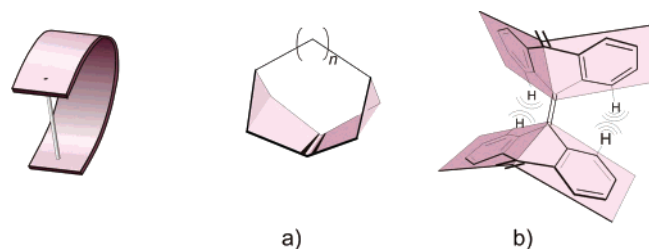


Figure 36. Two strategies to pyramidalize a double bond. In the tricyclic system (a), pyramidalization is induced by ring strain, and in the bianthraquinodimethane (b), pyramidalization is enforced by the steric hindrance of the “inner” hydrogen atoms. To avoid sterical strain, the bianthraquinodimethane (b) could also twist the anthracene units with respect to each other or pyramidalize the central double bond in a trans configuration. According to our observations, however, cis pyramidalization is preferred in cyclic bianthraquinodimethanes (see text).

steric hindrance on the convex side to pyramidalize the double bond is more promising. Cyclic bianthraquinodimethanes exhibit a pyramidalized, olefinic bond (Figure 36b). The central double bond cannot be planar because of the steric hindrance of the inner ortho hydrogen atoms. A distortion from syn to anti pyramidalization (as, e.g., in bianthraquinodimethane) is prevented by the cyclic structure.^{58,98–102}

To connect the pyramidalized building block and the normal π part to construct the Möbius ring, the ring enlargement metathesis method was chosen (Figure 37).

Metathesis of a beltlike, in-plane conjugated ring and a “normal” annulene should result in a larger ring of either Hückel or Möbius topology. The Möbius ring should be preferred because it should be less strained, if the pyramidalized part (magenta in Figure 37) is preoriented as outlined above. The principle can be demonstrated with a simple cardboard or steelplate model (Figure 38).

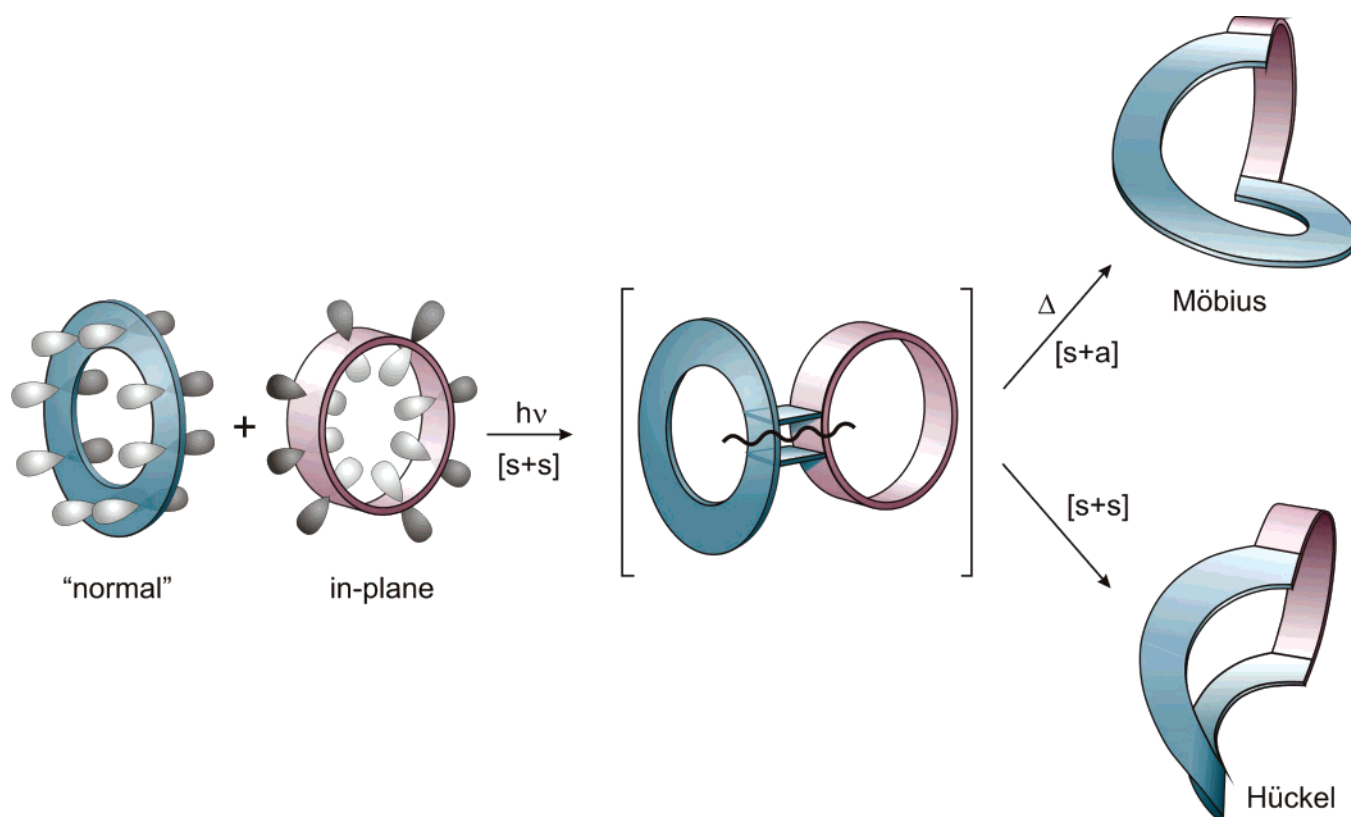


Figure 37. Ring enlargement metathesis as the strategy to connect a pyramidalized building block (magenta, beltlike system) with a normal conjugated π system (cyan, normal annulene) to form a Möbius ring. Portions of this figure are reprinted with permission from ref 93. Copyright 2006 Wiley-VCH.

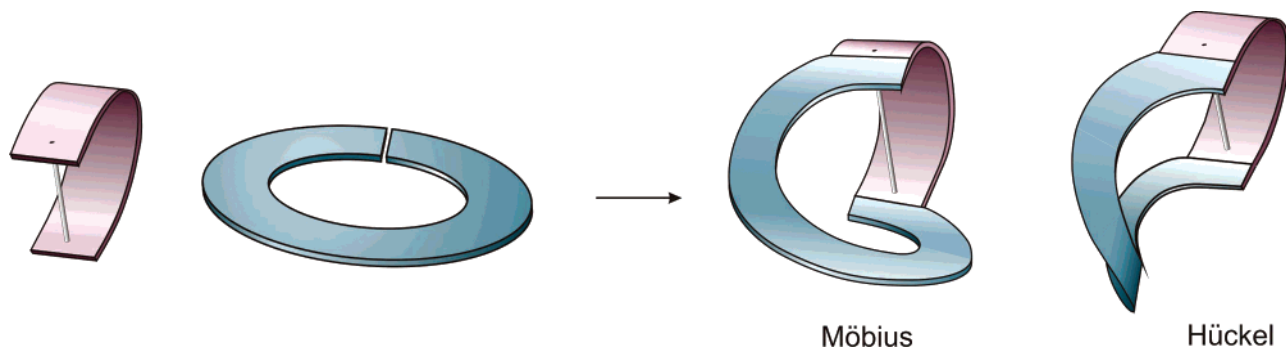


Figure 38. “Cardboard” or “steel plate model” to demonstrate that a Möbius ring is less strained, if a “pre-stressed” pyramidalized building block (magenta) is used as one of the components. Portions of this figure are reprinted with permission from ref 93. Copyright 2006 Wiley-VCH.

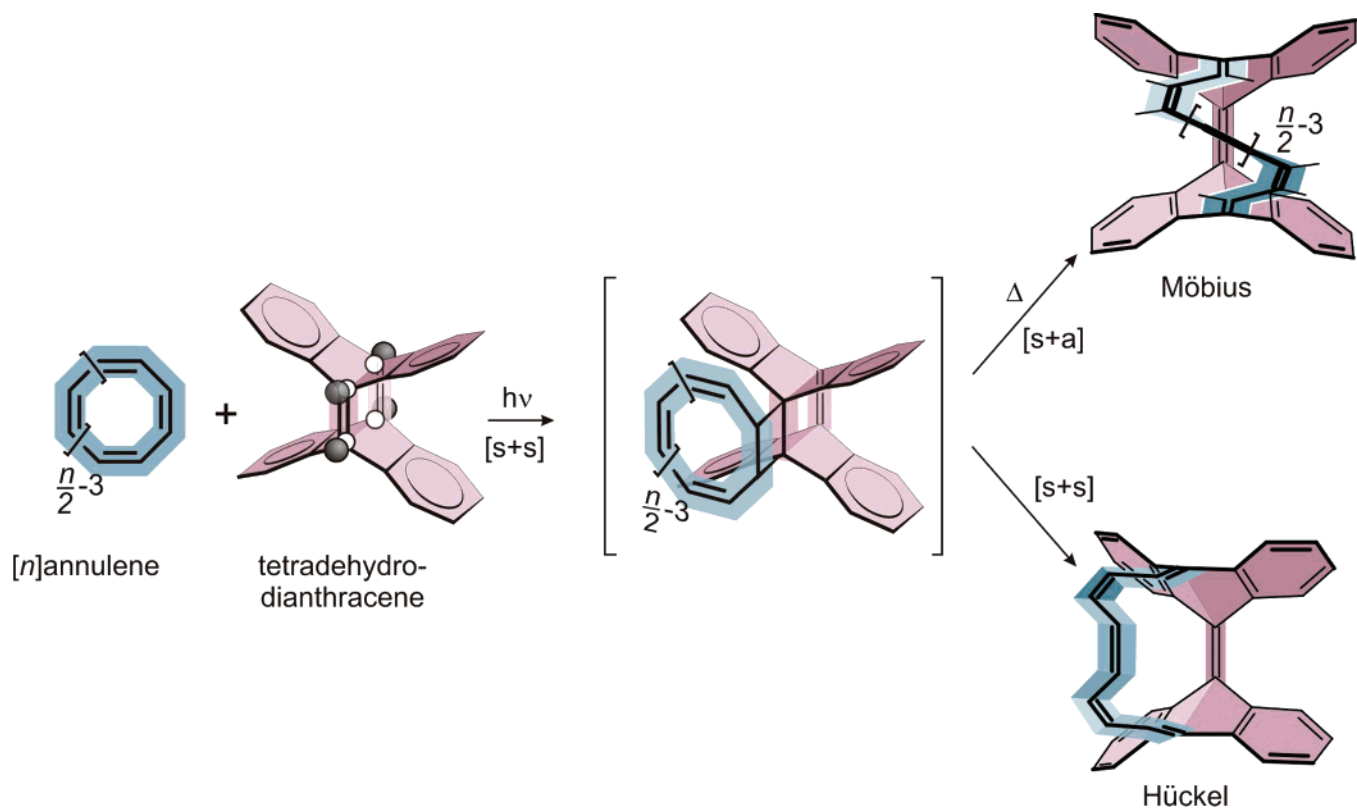


Figure 39. Synthetic approach to the preparation of a Möbius annulene by ring enlargement metathesis using tetrahydrodianthracene as the beltlike, pyramidalized component. The bianthraquinodimethane unit (magenta in the two products) should favor the formation of the Möbius isomer because it stabilizes the pyramidalized part of the Möbius annulene. Portions of this figure are reprinted with permission from ref 93. Copyright 2006 Wiley-VCH.

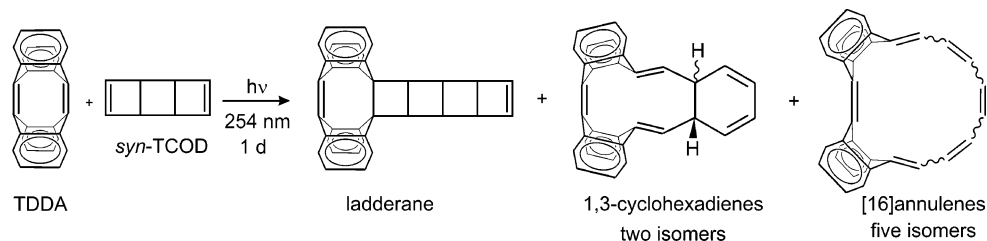


Figure 40. Photochemically induced metathesis reaction of tetrahydrodianthracene (TDDA) with *syn*-tricyclooctadiene.

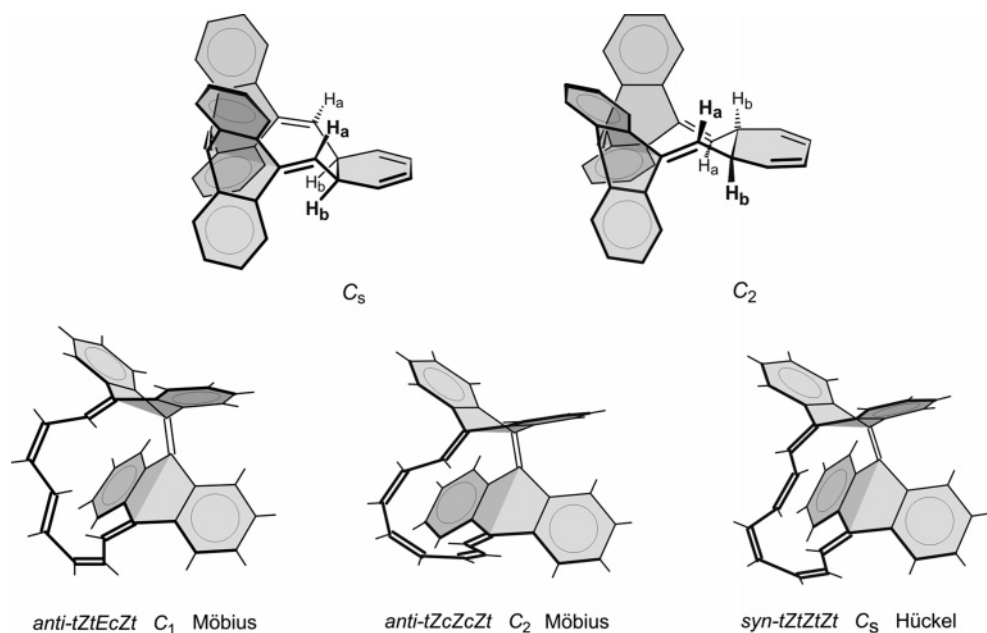
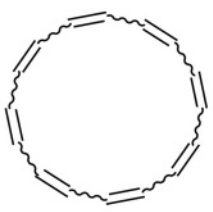
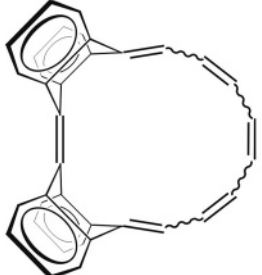


Figure 41. X-ray structures of the metathesis products of TDDA with TCOD (see Figure 40).

Table 2. Relative Energies (B3LYP/6-31G*, kcal mol⁻¹ and KMLYP/6-31G*) of the 20 Most Stable Isomers of Parent [16]Annulene (Left) and Bianthraquinodimethane-Modified [16]Annulene (Right)



parent [16]annulene



bianthraquinodimethane modified [16]annulene

parent [16]annulene					bianthraquinodimethane modified [16]annulene					
entry	E _{rel} ^{a)}	To po-logy ^{b)}	Configuration ^{c)}	^{d)}	entry	E _{rel} ^{a)}	E _{rel} ^{c)}	To po-logy	Configuration ^{d)}	^{d)}
1.	0.00	H	0011001100110011	X	1.	0.00	0.00	M	<i>syn-t Zc Zc Et</i>	N
2.	2.25	H	0011011011001111	N	2.	0.29	1.75	M	<i>anti-t Ec Zc Et</i>	?
3.	4.68	H	0001100110011011		3.	0.56	0.30	M	<i>syn-c Zt Ec Zt</i>	
4.	5.14	M	0000110011000111		4.	0.56	0.89	M	<i>syn-c Et Zc Zt</i>	
5.	5.15	M	0000111000110011		5.	2.47	4.95	M	<i>anti-c Et Zc Et</i>	
6.	5.41	M	0001100110011001		6.	2.76	1.96	M	<i>anti-t Zt Ec Zt</i>	X
7.	5.41	M	0001001100110011		7.	2.77	1.90	M	<i>anti-t Zc Zc Zt</i>	X
8.	5.45	H	0011011011011011		8.	4.16	3.26	H	<i>syn-t Ec Zc Et</i>	
9.	5.45	H	0011011001101111		9.	6.71	5.23	M	<i>syn-t Zc Zc Ec</i>	
10.	5.47	H	0011011001111011		10.	6.91	5.29	H	<i>syn-t Zt Zt Zt</i>	X
11.	5.83	H	0001100110011011		11.	8.36	10.74	M	<i>anti-t Ec Et Zc</i>	
12.	5.84	H	0001101100110011		12.	9.30	8.86	M	<i>syn-t Et Zc Zc</i>	
13.	6.03	H	0001101100110101		13.	9.34	13.06	M	<i>anti-c Et Zt Ec</i>	?
14.	6.05	H	0001010110011011		14.	11.20	10.25	M	<i>anti-t Zt Zc Zc</i>	
15.	6.22	M	0001001100110011		15.	11.20	10.25	M	<i>anti-c Zc Zx Zc</i>	
16.	6.24	H	0011001111001111		16.	11.74	11.56	H	<i>syn-c Et Zt Ec</i>	
17.	6.37	H	0001111001100101		17.	12.38	9.53	M	<i>syn-c Zt Zc Zc</i>	
18.	6.38	H	0001010011001111		18.	12.38	9.53	M	<i>syn-c Zc Zt Zc</i>	
19.	6.84	H	0001011100011011		19.	14.25	13.96	M	<i>syn-c Zt Ec Ec</i>	
20.	6.85	H	0001101100010111		20.	16.20	15.00	M	<i>syn-c Ec Zc Zc</i>	

^a B3LYP/6-31G*, ^b H (Hückel), M (Möbius). ^c 0 (Z), 1 (E). ^d Experimental characterization, X (X-ray), N (NMR), ? (ambiguous assignment to either entry 2 or entry 13). ^e KMLYP/6-31G*. ^f Syn/anti defines the relative stereochemistry of the two quinoid double bonds in the 9,10'-position of the quinodimethane unit. *t* (*s-trans*), *c* (*s-cis*), *E*, and *Z* refer to the stereochemistry in the polyene bridge.

To check whether the simple “cardboard model prediction” would hold in a “real” molecular system, we investigated the metathesis reaction of cyclooctatetraene with tetrahydrodianthracene, which should furnish a [16]annulene including a (“Möbius-stabilizing”) bianthraquinodimethane unit (Figure 39), and compared it with the parent [16]annulene.

Our calculations at the B3LYP/6-31G* level of DFT confirm the two known Hückel structures being the most stable isomers of unsubstituted [16]annulene^{37–39} (Table 2, left). The list of the 20 most stable isomers of parent [16]annulene includes 5 Möbius rings, however, with higher energies. Within the 20 most stable isomers of the bianthraquinodimethane-modified [16]annulenes (Table 2, right), there are 17 Möbius structures, and, moreover, the 7 most stable isomers are Möbius rings. Hence, based on theoretical grounds, the synthesis of a stable Möbius annulene (following the bianthraquinodimethane strategy) should be feasible.

However, all attempts to react cyclooctatetraene with tetrahydrodianthracene (TDDA) (Figure 39) upon heating, catalysis (Grubb’s catalysts), and irradiation failed to give

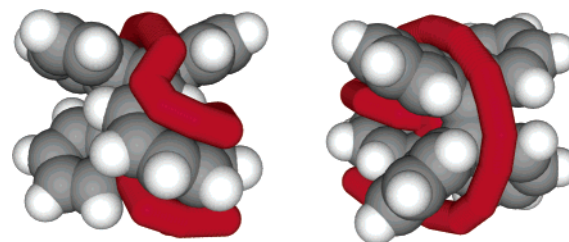


Figure 42. Two figures of the *anti-tZcZcZt* Möbius [16]annulene viewed from the front side and the back side. A “walk” on top of the annulene periphery (red tube) reveals that there is only one π surface. There is no inside and outside, and it takes two orbits to return to the starting point.

addition products. We isolated bianthryl as the main product instead. Further investigations revealed that, upon irradiation, cyclooctatetraene transferred triplet energy to the very low lying triplet state of TDDA, which in turn undergoes electrocyclic ring opening to the 9,10'-didehydrodianthracene

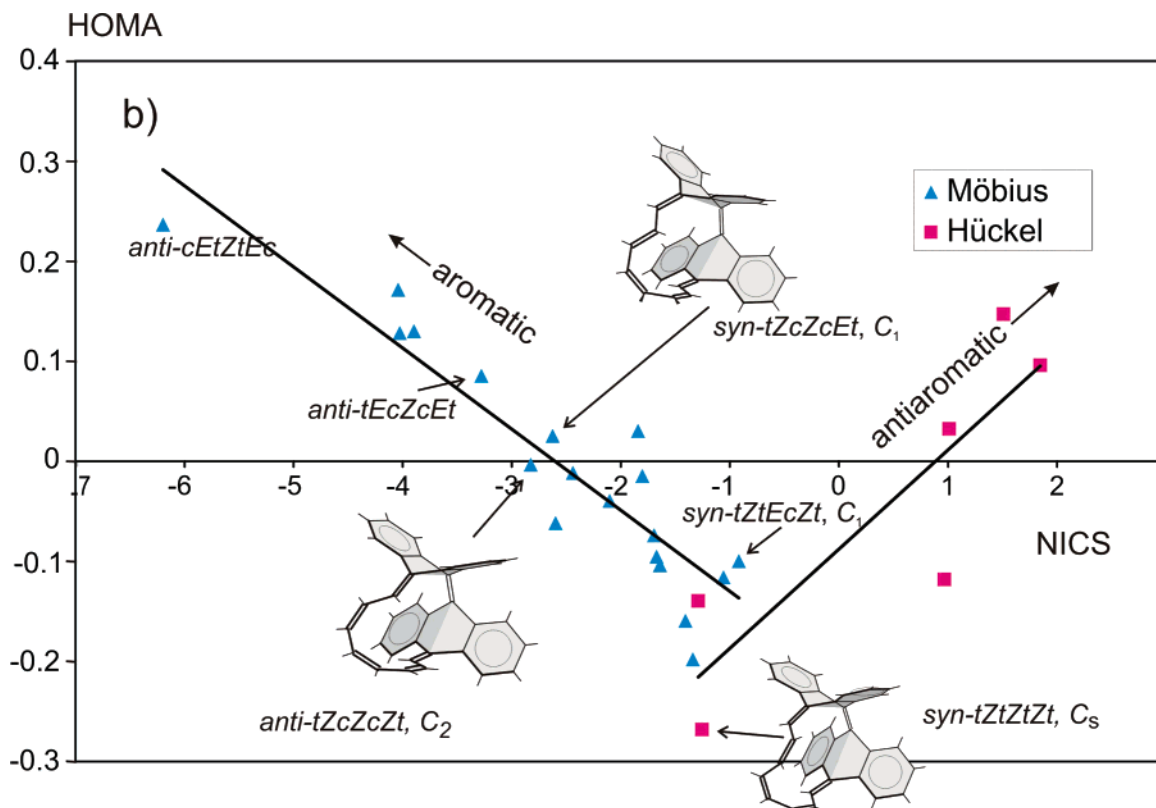


Figure 43. Aromaticity of the 25 most stable isomers of the bianthraquinodimethane-modified [16]annulene (Table 2, right). Two different aromaticity measures, the NICS value (GIAO, B3LYP/6-31G*) and HOMA (a quantitative measure of the bond length equalization), are plotted as a function of each other. Möbius isomers are marked with blue triangles and Hückel structures with pink squares. Aromatic molecules exhibit negative NICS values and large HOMA values. Isolated and characterized compounds are marked.



Figure 44. The logo of Renault is a double twisted band. Printed with permission from Renault-Nissan, Deutschland AG, Marketing Division.

diradical. To avoid these problems, we used *syn*-tricyclooctadiene (TCOD) as a masked cyclooctatetraene, which does not absorb UV light above 250 nm (Figure 40). Upon irradiation of TDDA with TCOD in benzene solution with a low-pressure mercury lamp, a ladderane, two 1,3-cyclohexadienes, and five ring-opened [16]annulene structures were isolated.

The two cyclohexadiene structures and three of the five [16]annulenes were characterized by X-ray structure analysis (Figure 41).

Anti-tZtEcZt (C_1 symmetry, entry 6, Table 2) and *anti-tZcZcZt* (C_2 symmetry, entry 7, Table 2) exhibit Möbius topology. *Syn-tZtZtZt* (C_s symmetry, entry 10, Table 2) is not twisted (Hückel topology). The global minimum (*syn-tZcZcEt*, C_1 symmetry, entry 1, Table 2) was characterized by NMR. In contrast to the other isomers, it is not stable at

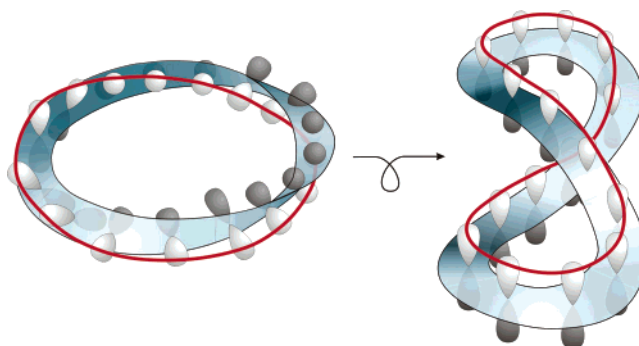


Figure 45. Topological transformation of a planar double twisted annulene into a “figure eight”-shaped annulene. Portions of this figure are reprinted with permission from ref 105. Copyright 2006 Wiley-VCH.

room temperature but undergoes a symmetry allowed electrocyclic ring closure to form the C_s symmetric 1,3-cyclohexadiene structure (Figure 41). Another isomer with Möbius topology could not be unambiguously assigned. According to the NMR data, it is either *anti-tEcZcEt* (entry 2, Table 2) or its conformer *anti-cEtZtEc* (entry 13, Table 2). The X-ray structures (Figure 41) and the geometries obtained by our DFT calculations (Table 2) are in excellent agreement.

The C_2 *anti-tZcZcZt* Möbius annulene forms yellow solutions in organic solvents and red crystals of trapezoid shape. It is indefinitely stable under ambient conditions in the dark. The crystals contain both enantiomers. Separation of the enantiomers was achieved by HPLC on a chiral stationary phase. All C–C bonds are conjugated; however, there is only one π surface. “Walking” above the [16]-

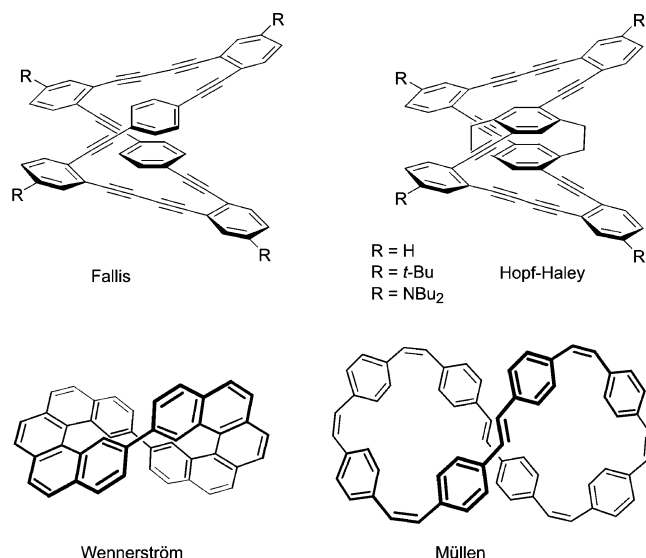


Figure 46. The propeller-type cyclophanes could be viewed as double twisted annulenes.

annulene periphery takes two rounds to return to the starting point. Also, in contrast to “normal” annulenes, every point on the molecular surface is accessible without leaving the π plane. There is no “inside” and “outside” of the ring, because both sides of the bianthraquinodimethane unit are connected with each other via the conjugated polyene bridge (Figure 42).

With their 16-electron periphery, the Möbius annulenes should be aromatic. Unfortunately, the four benzene rings reduce the Möbius aromaticity, albeit not to zero, as stated in a recent theoretical paper.¹⁰³ Aromaticity properties are distinctively different in the twisted (Möbius) as compared to the untwisted (Hückel) isomers. Möbius isomers exhibit an inverse correlation of NICS³⁵ and HOMA,³⁶ and a positive NICS/HOMA correlation is observed in Hückel structures. The more pronounced is the bond length equalization (large HOMA), the stronger is the paratropic ring current (large NICS). These relationships, which we already found in the parent [16]annulene (Figure 18), are also valid for the bianthraquinodimethane-modified [16]annulenes. According to the HOMA/NICS plot (Figure 43), *syn-tZtZt*, C_s (Hückel topology) is nonaromatic. Two of the dihedral angles in the polyene bridge are 103° . Obviously, this Hückel structure tries to escape antiaromatic destabilization by switching off conjugation (a structure with a dihedral angle of 90° would be neither Hückel nor Möbius). The global minimum of all bianthraquinodimethane-stabilized [16]annulenes (*syn-tZcZcEt*, C_1 , entry 1, Table 2), the C_2 symmetric *anti-tZcZcZt* Möbius structure (entry 7), as well as the isomers *anti-tEcZcEt* (entry 2) and *anti-cEtZtEc* (entry 13) are clearly on the best fit straight line of the aromatic structures (Figure 43).

It is probably not a simple endeavor to synthesize neutral Möbius annulenes with an aromaticity comparable to Hückel annulenes such as benzene. Most of the measures to stabilize the twist reduce the conjugation.

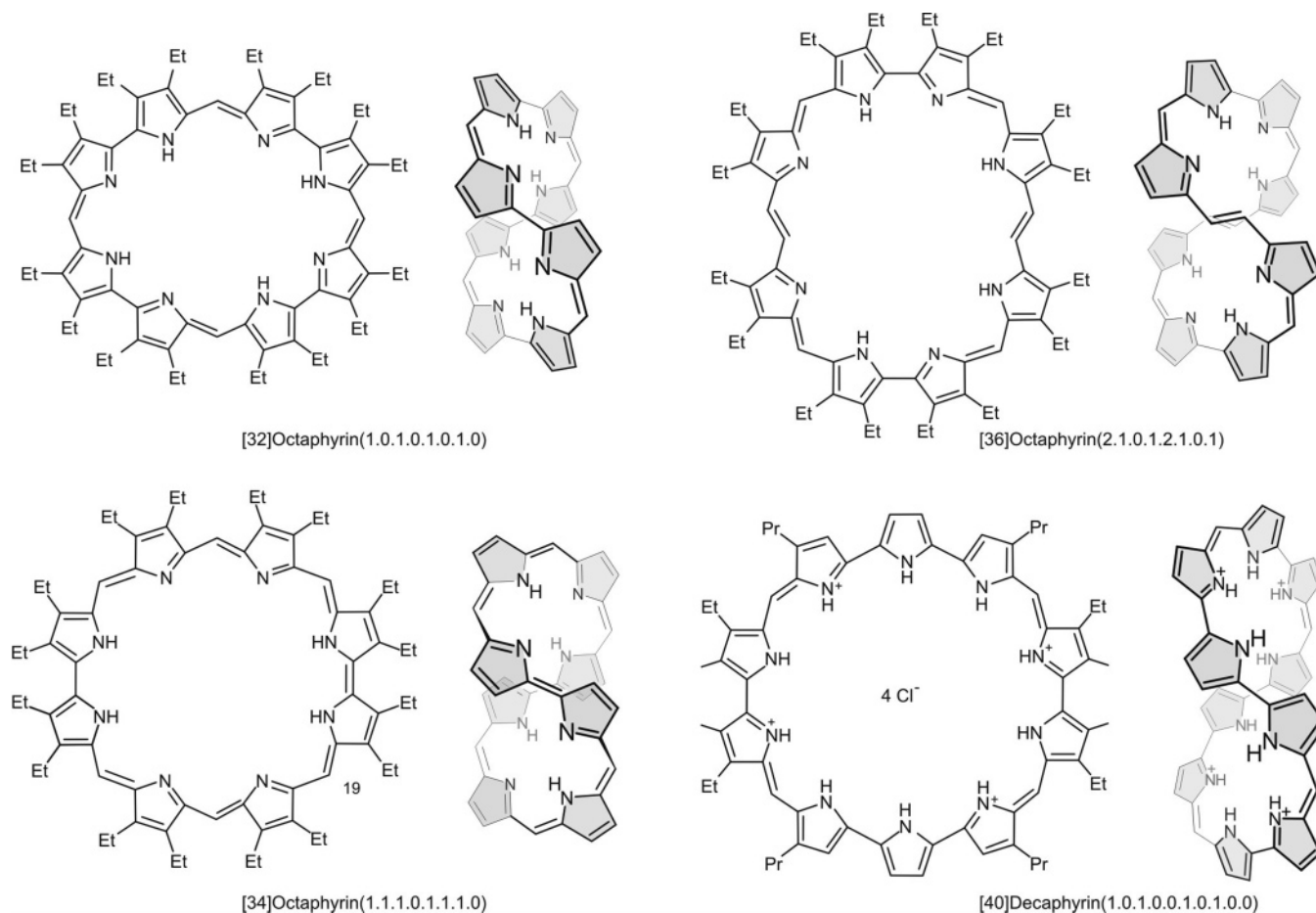


Figure 47. The known octa- and decaphyrins prefer a “figure eight”, double twisted configuration (structures with gray shaded pyrrole rings) over a planar non-twisted geometry.

4. Double Twisted π Systems

There are two different topological classes of twisted bands, those with an odd number of 180° twists that are one-sided and non-orientable and those with an even number of twists (two-sided and orientable) (Figure 44). All strips with an even number of 180° twists should follow the Hückel rule (aromatic with $4n+2$ electrons), and all bands with an odd number of twists are “anti-Hückel” systems. Even though they are both two-sided and orientable, a non-twisted and a double twisted band behave differently if being cut lengthwise. The non-twisted band yields two separate rings, and the double twisted band gives two rings that are concatenated (Figure 10, middle, Figure 12, bottom, Table 1).

Annulenes cannot be “cut down in the middle”, because the periphery is defined by only one edge, the C–C bonds. To visualize a double twist in an annulene, we define the twisted surface by the π nodal plane with the p orbitals as normal vectors on that surface (Figure 45). If we transform a planar, double twisted annulene into a “figure eight”-shaped system without interrupting the overlap of the p orbitals (assuming “rubber bonds”, red curve in Figure 45), the p orbitals become almost aligned and the double twist is difficult to recognize at a first glance. Most double twisted rings, such as a corresponding strip of paper, take a “figure eight” shape to reduce strain. In contrast to Möbius annulenes with a 180° twist, the larger 360° twist (paradoxically) does not induce much strain in a large enough annulene if the ring takes a “figure eight” shape.

It might seem strange that a double twisted annulene can have all p orbitals parallel with respect to each other (Figure 45, right), but if we accept the above definition, there are a few twisted annulenes experimentally known.^{104–107} The Fallis and Hopf–Haley cyclophanes (Figures 46 and 47) exhibit a 32π electron periphery and thus would be antiaromatic. However, the benzene rings drastically reduce the contiguous conjugation. Wennerström’s “propellicene” includes a [32]annulene (or a [16]annulene in the “inner” periphery) and Müllen’s [28]paracyclophane octaene a [48]-annulene perimeter. The latter was reduced to a hexaanion with a 54π electron diatropic system. However, it is not clear whether the “figure eight” conformation is retained.

“Regular” porphyrins include four pyrrole subunits, which are connected by four methine bridges. In corroles, one of the methane bridges is missing and the pyrrole rings are directly linked.¹⁰⁸ The bond angles of these porphyrinoid [18]-annulenes are close to the ideal bond angles of sp^2 hybridized carbon and nitrogen. Larger “expanded” porphyrins avoid the widening of the bond angles by introducing trans double bonds in the bridges and keep their structure approximately planar (e.g., [22]porphyrin(3.1.3.1), [22]porphyrin(2.2.2.2), [26]porphyrin(5.1.5.1), [34]porphyrin(5.5.5.5), [24]hexaphyrin(1.0.0.1.0.0)).¹⁰⁹ Porphyrins with 8 or 10 pyrrole rings and ring sizes from 32 to 40 (shortest conjugated path) reduce their bond angle strain by a double twist and by adopting a chiral “figure eight” geometry (Figure 47).

[34]Octaphyrin(1.1.1.0.1.1.1.0) and [36]octaphyrin-(2.1.0.1.2.1.0.1) do not racemize at room temperature in solution¹¹⁰ and could be separated into their enantiomers.¹¹¹ [32]Octaphyrin(1.0.1.0.1.0.1.0)¹¹² and [40]decaphyrin-(1.0.1.0.0.1.0.1.0.0)¹¹³ are dynamic structures. The two enantiomers rapidly interconvert at room temperature. The exact mechanism of the racemization is not known. However, because one enantiomer is clockwise double twisted and the other in an anticlockwise direction, four cis–trans isomer-

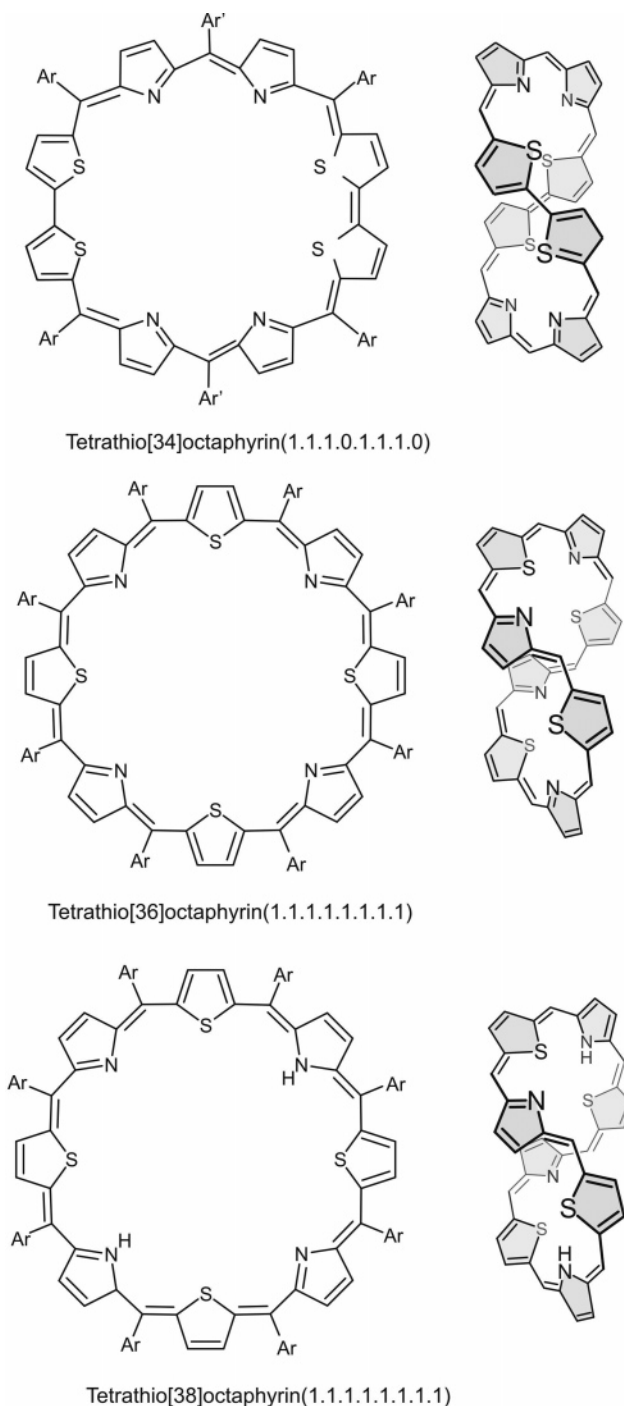


Figure 48. Double twisted heterooctaphyrins.

izations are required for racemization. The bonds that rotate are those that cross in the center of the “figure eight”, in Figure 47.

According to the Hückel rule (which is still valid for double twisted annulenes), the [34] porphyrin should be aromatic, and the [32]-, [36]-, and [40]porphyrins are antiaromatic. In the original papers and in reviews, the extended porphyrins in Figure 47 are termed “nonaromatic” because there are no abnormal chemical shifts in the ^1H NMR spectrum that would indicate a diatropic or paratropic ring current. However, as already discussed in the case of the C_2 symmetric Möbius [18]annulene (Figures 20 and 21), the lack of an up- or downfield shift of the meso protons does not imply that there is no ring current. The otherwise

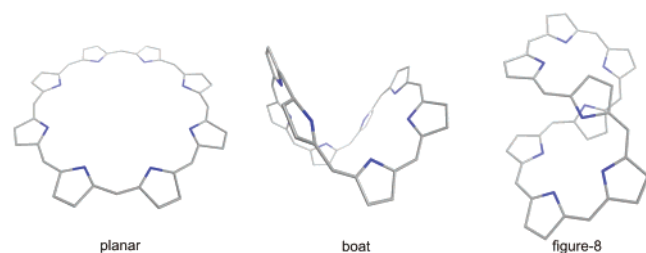


Figure 49. AM1 calculated geometries of octaphyrin in planar, boat, and “figure eight” geometry. In the “figure eight” conformation, the bond angles are closest to the linear octapyrrole and the ring strain therefore is minimized. The boat structure is probably the transition state of the racemization of the chiral “figure eight” structure.

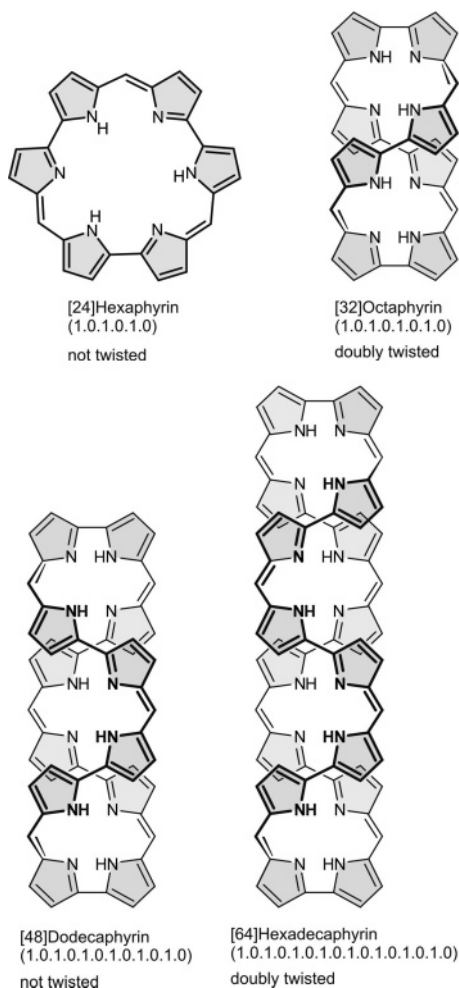


Figure 50. Extended porphyrins synthesized by Setsune et al. Ethyl groups in β and aryl substituents in meso positions are not shown for clarity.

indicative protons in the periphery of the porphyrins are approximately located between the shielding and deshielding range of the macrocyclic ring current in double twisted porphyrins, and therefore ring current effects on protons in the periphery are expected to be absent or small.

Some expanded hetero-octaporphyrins also exhibit double twisted “figure eight” topologies (Figure 48). Chandrasekhar et al. synthesized a [34]octaphyrin in which four of the pyrrole rings are replaced by thiophene. They term their compound aromatic, based on the downfield shifted signals of the β C–H protons.¹¹⁴ Latos-Grazynski and Sprutta prepared an interesting [36]octaphyrin, which was hydroge-

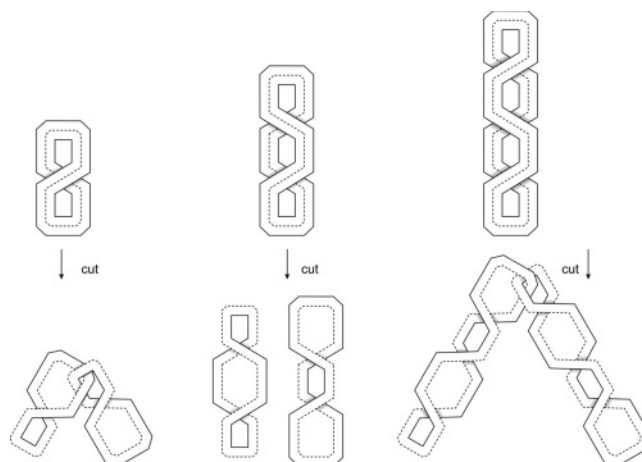


Figure 51. The twist in extended porphyrins can be demonstrated by cutting “model-porphyrins” lengthwise along the dashed line. In each case, two rings are formed. They are separate in non-twisted porphyrins and concatenated if double twisted porphyrins are cut.

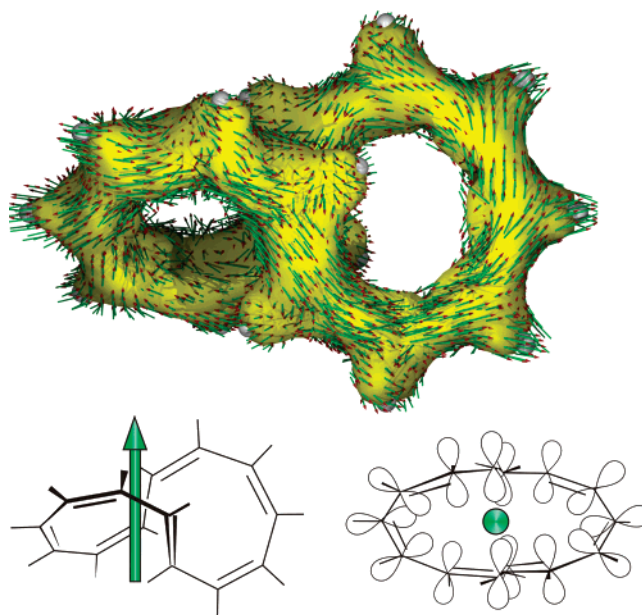


Figure 52. Theoretically predicted [14]annulene with a double twist.

nated to a [38]octaphyrin.¹¹⁵ A comparison of the ^1H NMR shifts was interpreted as an indication of a paratropic ring current in the 36 π electron system and a diatropic ring current in the 38 π electron macrocycle.

It is probably no coincidence that the double twisted form of porphyrins is preferred if the ring includes 8 or 10 five-membered rings and a conjugated path of 32–40 π electrons. Hypothetical planar octaphyrin(1.1.1.1.1.1.1.1) exhibits an average C–C–C bond angle at the methine bridges of about 146° , resulting in a considerable amount of ring strain (Figure 49).

The ring strain is smaller in the boat geometry and further reduced by distortion to the “figure eight” conformation. The latter combines favorable C–C–C bond angles in the macrocycle, which are close to the unstrained linear octapyrrole ($\sim 127^\circ$), and small dihedral angles that allow an efficient conjugation. The boat conformation most probably is the transition state of the racemization of both enantiomers of the “figure eight” form.

Larger expanded porphyrins form double twisted and untwisted rings in an alternating sequence with an increasing number of pyrrole rings included in the macrocycle. Setsune et al. synthesized the series of hexa-, octa-, dodeca-, and hexadecaporphyrins (Figure 50).¹¹⁶

The [24]hexaphyrin and [48]dodecaphyrin are not twisted, and [32]octaphyrin and [64]hexadecaphyrin are double twisted. The double twist can be demonstrated if a corresponding model is cut lengthwise as shown in Figure 51. The yield of larger porphyrins was increased by introducing larger substituents at the meso positions. Very large substituents in the meso position are obviously able to enforce a planar geometry in octaphyrins.¹¹⁷

Parent annulenes with a double twist are not known experimentally. Rzepa proposed a [14]annulene that based on theoretical calculations should be quite aromatic (NICS -18.3 and an almost perfect bond length equalization).¹¹⁸ The ACID calculation also predicts a perfectly conjugated system. If a magnetic field is applied parallel to one of the C_2 axes (Figure 52), a strong diatropic ring current is induced. Unlike normal planar annulenes, the p orbitals are in-plane in this projection (see also Figure 20). The structure could therefore be viewed as in-plane aromatic. Higher twisted annulenes¹¹⁹ and transition states¹²⁰ might also be conceivable.

5. References

- The oldest example to our knowledge is the retrograde canon "Ma fin est mon commencement" written by the medieval composer Guillaume de Machaut (1300–1377).
- Slonimsky, N. "The Moebius Strip-Tease". A perpetual canon written on a Möbius band to be revolved around the singer's head, which reads as follows: Ach! Professor Möbius, glöriöus Möbius / Ach, we love your topological, / And, ach, so logical strip! / One-sided inside and two-sided outside! / Ach! euphörius, glörius Möbius Strip-Tease!
- Möbius, A. F. Über die Bestimmung des Inhaltes eines Polyeders. *Berichte über die Verhandlungen der Königlich Sächsischen Gesellschaft der Wissenschaften zu Leipzig*; Sitzung am 27, November 1865; Vol. 17, pp 31–68.
- Listing, J. B. Der Census räumlicher Komplexe oder die Verallgemeinerung des Euler'schen Satzes von den Polyedern. *Abhandlungen der Mathematischen Classe der Königl. Gesellschaft der Wissenschaften zu Göttingen*; vorgetragen am 7, Dez. 1861; Vol. 10, pp 97–182.
- J. B. Listing was born in 1808 in Frankfurt, received his doctorate in 1834 with Carl Friedrich Gauss, and was appointed professor of physics in Göttingen in 1839. He made a remarkable range of contributions in different areas and coined a number of terms such as topology, entropic phenomena, nodal points, etc. His career progressed in a straightforward manner until he married Pauline Elvers in 1846. The couple immediately had financial problems, and on one occasion they were saved from bankruptcy by a friend in the Hannover ministry. Listing's standing in the scientific community was harmed by these problems, and he certainly received less recognition for his scientific achievements because of it. Breitenberger, E.; Listing, J. B. In *History of Topology*; James, I. M., Ed.; North-Holland: Amsterdam, 1999; pp 909–924.
- "Zur Theorie der Polyeder und der Elementarverwandschaft", *diaria mathematica*, Möbius, A. F. 1858, see also §11 of the "Preisarbeit" which was sent to Paris in 1861.
- Boy, W. *Math. Ann.* **1903**, 57, 151.
- Klein, F. Über Riemann's Theorie der algebraischen Functionen und ihrer Integrale, Teubner, Leipzig, 1882; p 80.
- Herges, R. *Naturwiss. Rundsch.* **2005**, 58, 301.
- Locher, J. L.; et al. *Die Welten des M. C. Escher*; Manfred Pawlak Verlagsgesellschaft: Herrsching, 1971.
- U.S. Patent 3,267,406, Aug 16, 1966.
- Walba, D. M.; Richards, M.; Haltiwanger, R. C. *J. Am. Chem. Soc.* **1982**, 104, 3219.
- Walba, D. M.; Homan, T. C.; Richards, R. M.; Haltiwanger, R. C. *New J. Chem.* **1993**, 17, 661.
- Frisch, H. L.; Wasserman, E. *J. Am. Chem. Soc.* **1961**, 83, 3789.
- Qubits (the logic states in a hypothetical quantum computer) must be addressable through external signals; however, they must not interact with the environment to prevent decoherence. Topological qubits were proposed as a superior implementation of quantum information. For a practical implementation, the molecules probably are too large and they lack an efficient isomerization mechanism between Möbius and non-Möbius. Ioffe, L. B.; Feigl'man, M. V.; Iosevich, A.; Ivanov, D.; Troyer, M.; Blatter, G. *Nature* **2002**, 415, 503.
- From Mathworld, <http://mathworld.wolfram.com/MoebiusStrip.html>.
- Van Gulick, N. *New J. Chem.* **1993**, 17, 619.
- Qui, W.-Y.; Xin, H.-W. *J. Mol. Struct. (THEOCHEM)* **1997**, 401, 151.
- Seifert, H. *Math. Ann.* **1935**, 110, 571.
- Köhler, H.; Dieterick, D. "Verfahren zur Herstellung von Verbindungen mit ineinandergeschlungenen Ringen". German Patent 1,069,617 (Nov. 26, 1959).
- Heilbronner, E. *Tetrahedron Lett.* **1964**, 1923.
- Hückel, E. *Z. Z. Phys.* **1931**, 70, 204.
- Hückel, E. *Z. Z. Phys.* **1932**, 76, 628.
- Zimmerman, H. E. *J. Am. Chem. Soc.* **1966**, 88, 1564.
- Frost, A. A.; Musulin, B. *J. Chem. Phys.* **1953**, 21, 572.
- Wannere, C. S.; Sattelmeyer, K. W.; Schaefer, H. F., III; Schleyer, P. v. R. *Angew. Chem., Int. Ed.* **2004**, 43, 4200; *Angew. Chem.* **2004**, 116, 4296.
- Havenith, R. W. A.; van Lenthe, J. H.; Jenneskens, L. *Int. J. Quantum Chem.* **2001**, 85, 52.
- Johnson, R. P.; Daoust, K. J. *J. Am. Chem. Soc.* **1996**, 118, 7381.
- Johnson, R. P.; Di Rico, K. J. *J. Org. Chem.* **1995**, 60, 1074.
- Castro, C.; Isborn, C. M.; Karney, W. L.; Mauksch, M.; Schleyer, P. v. R. *Org. Lett.* **2002**, 4, 3431.
- Martin-Santamaria, S.; Lavan, B.; Rzepa, H. S. *J. Chem. Soc., Perkin Trans. 2* **2000**, 1415.
- Balaban, A. T.; Banciu, M.; Ciorba, V. *Annulenes, Benzo-, Hetero-, Homo-Derivatives, and their Valence Isomers*; CRC Press, Inc.: Boca Raton, FL, 1987; Vol. 1, Chapter 4, p 67.
- Sondheimer, F. *Acc. Chem. Res.* **1972**, 5, 81.
- Kennedy, R. D.; Lloyd, D.; McNab, H. *J. Chem. Soc., Perkin Trans. 1* **2002**, 1601.
- Schleyer, P. v. R.; Maerker, C.; Dransfeld, A.; Jiao, H.; van Eikema Hommes, J. R. *J. Am. Chem. Soc.* **1996**, 118, 6317.
- Krygowski, T. M.; Cyranski, M. *Tetrahedron* **1996**, 52, 1713.
- Johnson, S. M.; Paul, I. C.; Geoffrey, S. D. *J. Chem. Soc. B* **1970**, 4, 643.
- Johnson, S. M.; Paul, I. C. *J. Am. Chem. Soc.* **1968**, 90, 6555.
- Oth, J. F. M.; Gilles, J.-M. *Tetrahedron Lett.* **1968**, 6259.
- Geuenich, D.; Hess, K.; Koehler, F.; Herges, R. *Chem. Rev.* **2005**, 105, 3758.
- Herges, R.; Geuenich, D. *J. Phys. Chem. A* **2001**, 105, 3214.
- Katz, T. J.; Garratt, P. J. *J. Am. Chem. Soc.* **1964**, 86, 5194.
- LaLancette, E. A.; Benson, R. E. *J. Am. Chem. Soc.* **1965**, 87, 1941.
- Barborak, J. C.; Su, T.-M.; Schleyer, P. v. R. *J. Am. Chem. Soc.* **1971**, 93, 279.
- Yakali, E. Genesis and bond relocation of the cyclononatetraenyl cation and related compounds. Dissertation, Syracuse University, 1973; p 39.
- Anastassiou, A. G.; Yakali, E. *J. Chem. Soc., Chem. Commun.* **1972**, 92.
- Anastassiou, A. G. The Cyclononatetraenyl Cation. *Topics in Nonbenzoid Aromatic Chemistry*; Wiley: New York, 1973; Vol. 1, p 18.
- Mauksch, M.; Gogonea, V.; Jiao, H.; Schleyer, P. v. R. *Angew. Chem., Int. Ed.* **1998**, 37, 2395.
- Mizoguchi, N. *Chem. Phys. Lett.* **1989**, 5, 383.
- Türker, L. *J. Mol. Struct. (THEOCHEM)* **1998**, 454, 83.
- Martin-Santamaria, S.; Rzepa, H. S. *J. Chem. Soc., Perkin Trans. 2* **2000**, 2378.
- Andre, J.-M.; Champagne, B.; Perpete, E. A.; Guillaume, M. *Int. J. Quantum Chem.* **2001**, 84, 608.
- Heilbronner, E. *Helv. Chim. Acta* **1954**, 37, 921.
- Aihara, J. *J. Chem. Soc., Perkin Trans. 2* **1994**, 971.
- Gutman, I.; Biedermann, P. U.; Ivanov-Petrovic, V.; Agranat, I. *Polycyclic Aromat. Compd.* **1996**, 8, 189.
- Choi, H. S.; Kim, K. S. *Angew. Chem.* **1999**, 111, 2400; *Angew. Chem., Int. Ed.* **1999**, 38, 2256.
- Houk, K. N.; Lee, P. S.; Nendel, M. *J. Org. Chem.* **2001**, 66, 5517.
- Herges, R. In *Conjugate Beltenes, in Modern Cyclophane Chemistry*; Hopf, H.; Gleiter, R., Eds.; VCH-Wiley: Weinheim, 2004; p 337.
- Kohnke, F. H.; Slawin, A. M. Z.; Stoddart, J. F.; Williams, D. J. *Angew. Chem.* **1987**, 99, 941; *Angew. Chem., Int. Ed. Engl.* **1987**, 26, 892.

- (60) Ashton, P. R.; Brown, G. R.; Isaacs, N. S.; Giuffrida, D.; Kohnke, F. H.; Mathias, J. P.; Slawin, A. M. Z.; Smith, D. R.; Stoddart, J. F.; Williams, D. J. *J. Am. Chem. Soc.* **1992**, *114*, 6330.
- (61) Ashton, P. R.; Girreser, U.; Giuffrida, D.; Kohnke, F. H.; Mathias, J. P.; Raymo, F. M.; Slawin, A. M. Z.; Stoddart, J. F.; Williams, W. J. *J. Am. Chem. Soc.* **1993**, *115*, 5422.
- (62) Cory, R. M.; McPhail, C. L.; Dikmans, A.; Vittal, J. J. *Tetrahedron Lett.* **1996**, 1983.
- (63) Cory, R. M.; McPhail, C. L. *Tetrahedron Lett.* **1996**, 1987.
- (64) Zoellner, R. W.; Krebs, J. F.; Browne, D. M. *J. Chem. Inf. Comput. Sci.* **1994**, *34*, 252.
- (65) Dobrowolski, J. *J. Chem. Inf. Comput. Sci.* **2002**, *42*, 490.
- (66) Diederich, F.; Staab, H. A. *Angew. Chem., Int. Ed. Engl.* **1978**, *17*, 372.
- (67) Staab, A. H.; Diederich, F. *Chem. Ber.* **1983**, *116*, 3487.
- (68) Craig, D. P.; Paddock, N. L. *Nature* **1958**, *181*, 1052.
- (69) Craig, D. P. *J. Chem. Soc.* **1959**, 997.
- (70) Rzepa, H. S. *Chem. Rev.* **2005**, *105*, 3697.
- (71) Martin-Santamaria, S.; Lavan, B.; Rzepa, H. S. *Chem. Commun.* **2000**, 1089.
- (72) Martin-Santamaria, S.; Rzepa, H. S. *J. Chem. Soc., Perkin Trans. 2* **2000**, 2372.
- (73) Rzepa, H. S.; Taylor, K. R. *J. Chem. Soc., Perkin Trans. 2* **2002**, 1499.
- (74) Herges, R. *Angew. Chem.* **1994**, *106*, 261; *Angew. Chem., Int. Ed. Engl.* **1994**, *33*, 255.
- (75) Herges, R. *J. Chem. Inf. Comput. Sci.* **1994**, *43*, 91.
- (76) Berger, C.; Bresler, C.; Dilger, U.; Geuenich, D.; Herges, R.; Röttele, H.; Schröder, G. *Angew. Chem.* **1998**, *110*, 1951; *Angew. Chem., Int. Ed. Engl.* **1998**, *37*, 1850.
- (77) Berger, C.; Dieterich, S.; Dilger, U.; Geuenich, D.; Helios, H.; Herges, R.; Kirchmer, P.; Röttele, H.; Schröder, G. *Angew. Chem.* **1998**, *110*, 1954; *Angew. Chem., Int. Ed. Engl.* **1998**, *37*, 1854.
- (78) Dilger, U.; Franz, B.; Röttele, H.; Schröder, G.; Herges, R. *J. Prakt. Chem.* **1998**, *340*, 468.
- (79) Herges, R.; Geuenich, D.; Bucher, G.; Tönshoff, C. *Chem.-Eur. J.* **2000**, *6*, 1224.
- (80) Kimball, D. B.; Herges, R.; Haley, M. M. *J. Am. Chem. Soc.* **2002**, *124*, 1572.
- (81) Kimball, B.; Weakley, T. J. R.; Herges, R.; Haley, M. M. *J. Am. Chem. Soc.* **2002**, *124*, 13463.
- (82) Shirliff, L. D.; Weakley, T. J. R.; Haley, M. M.; Köhler, F.; Herges, R. *J. Org. Chem.* **2004**, *69*, 6979.
- (83) Fowler, P. W. *Phys. Chem. Phys.* **2002**, *4*, 2878.
- (84) Dauben, H. J.; Wilson, J. D.; Laity, J. L. In *Nonbenzenoid Aromatics*; Snyder, J. P., Ed.; Academic Press: New York, 1971.
- (85) Moran, D.; Manoharan, M.; Heine, T.; Schleyer, P. v. R. *Org. Lett.* **2003**, *5*, 23.
- (86) Zimmerman, H. E. *Acc. Chem. Res.* **1971**, *4*, 272.
- (87) Dewar, M. J. S. *Angew. Chem.* **1971**, *83*, 859; *Angew. Chem., Int. Ed. Engl.* **1971**, *10*, 761.
- (88) Woodward, R. B.; Hoffmann, R. *Angew. Chem.* **1969**, *81*, 797; *Angew. Chem., Int. Ed. Engl.* **1969**, *8*, 781.
- (89) Herges, R.; Jiao, H.; Schleyer, P. v. R. *Angew. Chem., Int. Ed. Engl.* **1994**, *33*, 1376.
- (90) Jiao, H.; Schleyer, P. v. R. *J. Chem. Soc., Perkin Trans. 2* **1994**, 407.
- (91) Castro, C.; Karney, W. L.; Valencia, M. A.; Vu, C. M. H.; Pemberton, R. P. *J. Am. Chem. Soc.* **2005**, *127*, 9704.
- (92) Ajami, D.; Oeckler, O.; Simon, A.; Herges, R. *Nature* **2003**, *426*, 819.
- (93) Ajami, D.; Hess, K.; Köhler, F.; Näther, C.; Oeckler, O.; Simon, A.; Yamamoto, C.; Okamoto, Y.; Herges, R. *Chem.-Eur. J.* **2006**, *12*, 5434.
- (94) Sondheimer, F.; Gaoni, Y. *J. Am. Chem. Soc.* **1961**, *83*, 4863.
- (95) Schröder, G.; Oth, J. F. M. *Tetrahedron Lett.* **1966**, 4083.
- (96) Stevenson, C. D.; Kurth, T. L. *J. Am. Chem. Soc.* **1999**, *121*, 1623.
- (97) Borden, W. T. *Chem. Rev.* **1989**, *89*, 1095.
- (98) Kammermaier, S.; Herges, R. *Angew. Chem.* **1996**, *108*, 470; *Angew. Chem., Int. Ed. Engl.* **1996**, *35*, 417.
- (99) Kammermaier, S.; Jones, P. G.; Herges, R. *Angew. Chem.* **1996**, *108*, 2834; *Angew. Chem., Int. Ed. Engl.* **1996**, *35*, 2669.
- (100) Kammermaier, S.; Jones, P. G.; Herges, R. *Angew. Chem.* **1997**, *109*, 1825; *Angew. Chem., Int. Ed. Engl.* **1997**, *36*, 1757.
- (101) Kammermaier, S.; Herges, R. *Angew. Chem.* **1997**, *109*, 2317; *Angew. Chem., Int. Ed. Engl.* **1997**, *36*, 2200.
- (102) Herges, R.; Deichmann, M.; Grunenberg, J.; Bucher, G. *Chem. Phys. Lett.* **2000**, *327*, 149.
- (103) Castro, C.; Chen, Z.; Wannere, C. S.; Jiao, H.; Karney, W. L.; Mauksch, M.; Puchta, R.; Hommes, N. J. R. v. E.; Schleyer, P. v. R. *J. Am. Chem. Soc.* **2005**, *127*, 2425.
- (104) Collins, S. K.; Yap, G. P. A.; Fallis, A. G. *Org. Lett.* **2000**, *2*, 3189.
- (105) Hinrichs, H.; Boydston, A. J.; Jones, P. G.; Haley, M. M.; Hopf, H.; Hess, K.; Herges, R. *Chem.-Eur. J.* **2006**, *12*, 7103.
- (106) Thulin, B.; Wennerström, O. *Acta Chim. Scand.* **1976**, *B30*, 688.
- (107) Schenk, R.; Müllen, K.; Wennerström, O. *Tetrahedron Lett.* **1990**, *50*, 7367.
- (108) Montforts, F. P.; Glaserapp-Breiling, M.; Kusch, D. Porphyrins and related compounds. In *Houben-Weyl, Methods of Organic Chemistry*; Schaumann, E., Ed.; Georg Thieme Verlag Stuttgart: New York, 1998; Vol. E 9d, Hetarenes IV, p 577.
- (109) Montforts, F. P.; Glaserapp-Breiling, M.; Kusch, D. Porphyrins and related compounds. In *Houben-Weyl, Methods of Organic Chemistry*; Schaumann, E., Ed.; Georg Thieme Verlag Stuttgart: New York, 1998; Vol. E 9d, Hetarenes IV, p 687.
- (110) Vogel, E.; Bröring, M.; Fink, J.; Rosen, D.; Schmickler, H.; Lex, J. K.; Chan, W. K.; Wu, Y.-D.; Nendel, M.; Plattner, D. A.; Houk, K. N. *Angew. Chem.* **1995**, *107*, 2705; *Angew. Chem., Int. Ed. Engl.* **1995**, *34*, 2515.
- (111) Werner, A.; Michels, M.; Zander, L.; Lex, J.; Vogel, E. *Angew. Chem.* **1999**, *111*, 3866.
- (112) Bröring, M.; Jendry, J.; Zander, L.; Schmickler, H.; Lex, J.; Wu, Y.-D.; Nendel, M.; Chen, J.; Plattner, D. A.; Houk, K. N.; Vogel, E. *Angew. Chem.* **1995**, *107*, 2709; *Angew. Chem., Int. Ed. Engl.* **1995**, *34*, 2511.
- (113) Sessler, J. L.; Weghorn, S. J.; Lynch, V.; Johnson, M. R. *Angew. Chem.* **1994**, *106*, 1572; *Angew. Chem., Int. Ed. Engl.* **1994**, *33*, 1509.
- (114) Rath, H.; Sankar, J.; PrabhuRaja, V.; Chandrasekhar, T. K.; Joshi, B. S.; Roy, R. *Chem. Commun.* **2005**, 3343.
- (115) Sprutta, N.; Latos-Grazynski, L. *Chem.-Eur. J.* **2001**, *7*, 5099.
- (116) Setsune, J.-i.; Katakami, Y.; Iizuna, N. *J. Am. Chem. Soc.* **1999**, *121*, 8957.
- (117) Anand, V. G.; Pushpan, S. K.; Venkatraman, S.; Dey, A.; Chandrasekhar, T. K.; Joshi, B. S.; Roy, R.; Teng, W.; Senge, K. R. *J. Am. Chem. Soc.* **2001**, *123*, 8620.
- (118) Rzepa, H. S. *Org. Lett.* **2005**, *7*, 4637.
- (119) Rzepa, H. S. Private communication.
- (120) Rzepa, H. S. *Chem. Commun.* **2005**, 5220.

CR0505425